HAROKOPIO UNIVERSITY

School of Environment, Geography and Applied Economics
Geography Department

Postgraduate Programme "Applied Geography and Spatial Planning"
Stream C: Geoinformatics

Master Thesis

On the relationship between C-band SAR backscatter coefficient (sigma^0) and Above Ground Biomass (AGB) of mountainous Mediterranean forests with the use of Sentinel-1 satellite data: a preliminary approach

Maria Karamihalaki

Athens, September 2017

HAROKOPIO UNIVERSITY

School of Environment, Geography and Applied Economics

Geography Department

Postgraduate Programme "Applied Geography and Spatial Planning"

Stream C: Geoinformatics

Three – Member Committee

Issaak Parcharidis (Supervisor)
Associate Professor, Geography Department, Harokopio University

Vassilis Detsis (Co – supervisor)
Assistant Professor, Department of Home Economics and Ecology, Harokopio University

Stamatis Kalogirou
Assistant Professor, Geography Department, Harokopio University

I, Maria Karamihalaki, declare responsibly that:

1) I am the owner of the intellectual rights of this original thesis, and to the best of my knowledge, my thesis does not slander any physical persons, nor does it offend the intellectual rights of third parties.

2) I accept that the LIC may, without changing the content of my thesis, make it available electronically through its Digital Library, copy it in any medium and/ or any format and hold more than one copy for maintenance and safety purposes.

"Once a photograph of the Earth, taken from outside, is available,
once the sheer isolation of the Earth become known,
a new idea, as powerful as any in history,
will be let loose."

Sir Fred Hoyle, astronomer (1948).

ACKNOWLEDGEMENTS

I would like to express my gratitude to every single person who contributed to the current study, starting by the Associate Professor of the Geography Department, of Harokopio University, Dr. Issaak Parcharidis, who had the main supervision of this Master thesis. I would like to thank him, not only for supporting me through this study, but also for being a source of inspiration since my undergraduate studies, as he was the person who introduced me to the science and the art of monitoring the Earth from space. I would also like to acknowledge him as an excellent advisor and to thank him for our collaboration and for the many things I learned by his side. I would like to express my deep gratitude to the Assistant Professor of the Department of Home Economics and Ecology, of Harokopio University, Dr. Vassilis Detsis, who co-supervised this Master thesis. His contribution was highly important and had a great impact on this study, regarding his views on the subject, the discussions on the theoretical approach and the methodology, the field work and the analysis of the data. More importantly, I would like to thank him for our excellent collaboration, his patience with the great amount of questions and concerns that I had and his guidance through every single stage of this study. I would like to thank the Associate Researcher of the Institute for Astronomy, Astrophysics, Space Applications and Remote Sensing (IAASARS), of the National Observatory of Athens (NOA), Dr. Olga Sykioti, who is my former supervisor and the person who had the greatest impact on me as a researcher, so far. Our collaboration was of significant importance for me, as she showed me the way to research methodology and had a major contribution on the way that I consider science and research. I want to take the chance to thank my former research team; in particular I would like to thank the Associate Professor of the Department of Biological Applications and Technologies, of the University of Ioannina, Dr. Aris Kyparissis and the Postdoctoral Researcher of the Institute of Applied and Computational Mathematics (IACM), of the Foundation of Research and Technology – Hellas (FORTH), Dr. Stavros Stagakis, as they introduced me to the research field of the monitoring of terrestrial vegetated ecosystems' dynamics and vegetation phenology by means of remote sensing. Our collaboration acted for me as a factor that highly contributed to the formation of my current research interests. I would also like to express my gratitude to the Ph.D.

student Richard Crabbe, from the Global Change Research Institute, of the Czech Academy of Sciences, for his interesting views on the subject. Furthermore, I would like to thank the Assistant Researcher of the Forest Research Institute (FRI), of the Hellenic Agricultural Organization, Dr. Nikolaos M. Fyllas and his team, for having the kindness to provide us with their invaluable *in-situ* data, which had a significant contribution to the results of the current study. Lastly, I would like to thank all the scientists and the engineers who worked on the production and the development of the data, the algorithms and the methodologies used in this study. The input Sentinel – 1 GRD products are provided by the European Space Agency, under the European Commission's Copernicus Programme. The Sentinel Application Platform (SNAP) for the processing of the data is developed by the European Space Agency.

Table of Contents

Table of images

This page intentionally left blank

Preface

I find rather exciting how today's technology offers us the capacity to monitor our planet in so many different aspects and the fact that the main information used for this purpose is practically derived from space, makes it even better. I chose to use this technology as a tool, in order to study another thing that amazes me, which is the natural environment. Being part of a changing planet, is all the motivation that one needs to start wanting to study those changes. In an era where the term "climate change" sounds more like a cliché, rather than a phenomenon that needs to be understood and controlled, building environmental awareness within human communities, developing mechanisms for the sustainable management and exploitation of the environment and its natural resources and getting closer to understanding what this term actually means anyway, become even more challenging and even more necessary.

Carbon dioxide consists one of the major parameters affecting the global climate. In this Master thesis, a first, preliminary approach is attempted on the relationship between terrestrial carbon dioxide and satellite derived parameters. The main idea that surrounds the study of such relationships lies in the fact that when those relationships are finally established, we will then be able to monitor carbon dioxide from space, with the use of satellite data.

The main goal of this study was reached; the relationships between the studied parameters were examined and they are hereby presented, with respect to all the limitations driven by the methods and the data that were used. For me, however, the most important part of the current study was the effect that it had on me as a researcher and the way that it contributed to the evolution of my research interests and views.

Maria Karamihalaki, Athens, 2017

Abstract

Carbon monitoring in regional and global scales is of significant importance for the comprehension of the global carbon cycle. About 45% of the terrestrial carbon is stored into forest biomass; therefore, the development of methodologies and models for the monitoring and the quantification of Above Ground Biomass (AGB) in different types of forest ecosystems arises as a key mechanism for carbon monitoring. Satellite remote sensing techniques constitute a powerful and promising source of information, providing global data with spatial and temporal continuity. In order to proceed to the modeling and mapping of AGB, with the use of satellite remote sensing techniques, the relationship between AGB and satellite derived parameters has to be determined. In this study, a preliminary approach is being attempted on the relationship between C-band SAR backscatter coefficient ($sigma^0$) and AGB that was estimated from *in situ* data that were collected from four different Mediterranean conifer forests, of *Abies cephalonica* Loudon, in Greece. For the purposes of the study, *in-situ* data of forest structural parameters (DBH and tree height) were collected in the field and were then used in allometric equations, for the estimation of AGB. Sentinel – 1 GRD products were processed for the retrieval of the SAR backscatter coefficient ($sigma^0$) values. Two empirical models were then applied, for the investigation of the relationship between the *in-situ* measured AGB and the C – band SAR backscatter coefficient. First results demonstrate the existence of a moderate relationship between the VH polarized SAR backscatter coefficient, of the ascending pass of the satellite, and the AGB, while no significant relationship is found between either the VV polarized SAR backscatter coefficient of both passes, or the VH polarized SAR backscatter of the descending pass and the AGB.

Key words: carbon, Above Ground Biomass (AGB), Synthetic Aperture Radar (SAR), *Abies Cephalonica* Loudon, Sentinel – 1.

Abstract in Greek / Περίληψη στα ελληνικά

Η παρακολούθηση του άνθρακα σε τοπικές και παγκόσμιες κλίμακες είναι εξέχουσας σημασίας για την κατανόηση του κύκλου του άνθρακα. Περίπου το 45% του χερσαίου άνθρακα βρίσκεται αποθηκευμένος στη βιομάζα των δασικών οικοσυστημάτων· επομένως, η ανάπτυξη μεθοδολογιών και μοντέλων, για την παρακολούθηση, την εκτίμηση και την ποσοτικοποίηση της υπέργειας βιομάζας (Above Ground Biomass, AGB) για διαφορετικούς τύπους δασικών οικοσυστημάτων, αναδύεται ως ένας μηχανισμός κλειδί για την παρακολούθηση του άνθρακα. Οι τεχνικές δορυφορικής τηλεπισκόπησης αποτελούν μία ισχυρή πηγή πληροφορίας, η οποία παρέχει δεδομένα με χωρική και χρονική συνέχεια, σε παγκόσμια κλίμακα. Προκειμένου να προχωρήσει κανείς στην μοντελοποίηση και τη χαρτογράφηση της υπέργειας βιομάζας, με τη χρήση τεχνικών τηλεπισκόπησης, πρέπει να προσδιοριστεί η σχέση μεταξύ αυτής και παραμέτρων που προκύπτουν από δορυφορικά δεδομένα. Στην παρούσα μελέτη, επιχειρείται μία πρώτη, προκαταρκτική προσέγγιση, στη διερεύνηση της σχέσης μεταξύ του συντελεστή του οπισθοσκεδαζόμενου σήματος SAR (C-band) και της υπολογισθείσας από δεδομένα πεδίου υπέργειας βιομάζας. Τα δεδομένα πεδίου (*in-situ*) συλλέχθηκαν από δασικά οικοσυστήματα κεφαλληνιακής ελάτης (*Abies cephalonica* Loudon), σε τέσσερις διαφορετικές θέσεις στην Ελλάδα. Τα δεδομένα που συλλέχθηκαν στο πεδίο αφορούν δομικά χαρακτηριστικά των δέντρων και αναφέρονται συγκεκριμένα στη μέτρηση της στηθιαίας διαμέτρου (DBH) και του ύψους. Στη συνέχεια έγινε εισαγωγή των δεδομένων πεδίου σε αλλομετρικές εξισώσεις, για την εκτίμηση της υπέργειας βιομάζας. Ακόμα, έγινε χρήση των προϊόντων GRD, του δορυφόρου Sentinel – 1, του ευρωπαϊκού προγράμματος Copernicus, για την εξαγωγή των τιμών του συντελεστή οπισθοσκέδασης SAR ($sigma^0$). Δύο εμπειρικά μοντέλα εφαρμόσθηκαν στη συνέχεια, για τη διερεύνηση της σχέσης μεταξύ του συντελεστή οπισθοσκέδασης SAR και της υπολογισθείσας από δεδομένα πεδίου υπέργειας βιομάζας. Τα πρώτα αποτελέσματα υποδεικνύουν την ύπαρξη μιας μέτριου βαθμού σχέσης μεταξύ του οπισθοσκεδαζόμενου σήματος SAR, με πόλωση VH, για το ανοδικό πέρασμα του δορυφόρου της υπέργειας βιομάζας, ενώ καμία σημαντική συσχέτιση δεν βρέθηκε μεταξύ του οπισθοσκεδαζόμενου σήματος SAR με πόλωση VV (και για τα δύο περάσματα του δορυφόρου) και της υπέργειας βιομάζας, αλλά και μεταξύ του

οπισθοσκεδαζόμενου σήματος SAR, με πόλωση VH, για το καθοδικό πέρασμα του δορυφόρου και της υπέργειας βιομάζας.

Λέξεις κλειδιά: άνθρακας, υπέργεια βιομάζα (AGB), ραντάρ συνθετικού ανοίγματος (SAR), *Abies Cephalonica* Loudon, Sentinel – 1.

List of acronyms

AGB	Above Ground Biomass
ALOS – PALSAR	Advanced Land observation satellite – Phased array type L-band synthetic aperture Radar
DBH	Diameter at Breast Height
DN	Digital Number
EAA	European Environment Agency
EC	European Commission
ECV	Essential Climate Variable
EO	Earth Observation
ESA	European Space Agency
FRI	Forest Research Institute
GHG	Greenhouse Gases
GDR	Ground Range Detected
GPP	Gross Primary Production
GTOS	Global Terrestrial Observing System
IPCC	Intergovernmental Panel on Climate Change
JAXA	Japan Aerospace Exploration Agency
LULUCF	Land Use, Land-Use Change and Forestry
LUT	Look Up Tables
MMSE	Minimum Mean Square Error
NASA	National Aeronautics and Space Administration
NPP	Net Primary Production
RADAR	RAdio Detection And Ranging
REDD	Reduced Emissions from Deforestation and Degradation
RDB	Rwanda Development Board
SAR	Synthetic Aperture Radar
TOPSAR	Terrain Observation with Progressive Scans SAR
UNEP	United Nations Environment Programme
UNFCCC	United Nations Framework Convention on Climate Change
VH	Vertical – Horizontal
VV	Vertical – Vertical
WCMC	World Conservation Monitoring Centre

Definition and units of measure

According to the Global Terrestrial Observing System (GTOS), biomass is defined as mass of live or dead organic matter. Changes in time of vegetation biomass per unit area (biomass density) can be used as an *essential climate variable* (ECV), because they are a direct measure of sequestration or release of carbon between terrestrial ecosystems and the atmosphere (Bombelli et al., 2009). According to the IPCC Good Practice Guidance for LULUCF (2003), the carbon pools of terrestrial ecosystems involving biomass are conceptually divided into above-ground and below-ground biomass, dead mass and litter (Bombelli et al., 2009).

In this study, only the Above Ground Biomass (AGB) is being discussed. The use of the term "Above Ground Biomass", is referring to the mass of the stem, the branches and foliage of live tress with DBH (Diameter at Breast Height) > 4cm. AGB is measured in Mg/ ha (megagrams per hectare) and CO_2 is measured in Mg/ ha as well.

The SAR backscatter coefficient ($sigma^0$) is measured in db (decibel).

1. Introduction

Biogeochemical cycles of carbon are of vital importance for the ecosystems, as carbon is one of the major components and prerequisites for life, due to its significant structural role for both biotic and abiotic factors. During the last decades, this major chemical component has been having its popularity increased, owing to its role in the compound of carbon dioxide (CO_2). Given the fact that carbon dioxide is one of the major greenhouse gases, it is associated with global warming, climate change and environmental pollution. As carbon is the foundation of all life, balance is the key, and in order for it to be achieved, carbon monitoring has become one of the greatest necessities for environmental scientists. The scientific community focuses a great amount of its attention on forests, as forest ecosystems provide a significant sink for atmospheric CO_2. Forests play a vital role in regulating climate through carbon sequestration in their biomass (Sinha et al., 2015). Carbon concentrations in forests are directly related to the amount of biomass and therefore, the biggest the volume of a forest, the greatest its capacity as a carbon sink.

In an era of climate change, the significance of carbon monitoring invigorates. The scientific community agrees that increased concentrations of carbon dioxide, due to manmade carbon dioxide emissions, during the last century, has led to a series of environmental problems, that subsequently lead to increased mean temperature globally and extreme weather conditions regionally; shaped up together, these facts constitute a major component for climate change.

Being able to monitor and map the terrestrial biomass on a global scale is of great importance, as any activity that affects the amount of biomass in vegetation and soil has the potential to sequester carbon from, or release carbon into the atmosphere (Malhi et al. 2013). What is more, accurate estimates of forest (AGB), especially after anthropogenic disturbance, could reduce uncertainties in the carbon budget of terrestrial ecosystems and provide critical information to policy makers (Huang et al., 2015). In order to better understand the global biogeochemical carbon cycle, determining spatiotemporal variations in the carbon stock stored in forest biomass is important (Suzuki et al, 2013).

In situ measurements of structural forest parameters can provide accurate estimations of forest biomass. However, they lack the spatial and temporal extent needed to monitor this Essential Climate Variable in global scale. During the last decades, several models and techniques have been developed for the monitoring of carbon/ biomass in land vegetated ecosystems, with the use of satellite derived data (Chang and Shoshany, 2016, Huang et al., 2015, Suzuki et al., 2013, Morel et al., 2012, Sandberg et al., 2012, Lucas et al., 2010, etc.). Recently, there has been a growing interest in the use of microwave Synthetic Aperture Radar (SAR), for the estimation of AGB. SAR transmits a microwave pulse to the Earth's surface and receives the backscatter signal that is determined by the surface and includes information regarding the land surface structure, such as forest structural characteristics. (Suzuki et al, 2013). This attribute has demonstrated SAR data as an effective technological tool for AGB monitoring.

2. Literature review

Monitoring biomass of terrestrial ecosystems by means of remote sensing is being raised as a field of great interest for the scientific community, during the last years. On the review of related published studies, researchers explore the relationship between forest biomass and forest structural parameters and satellite derived features either from optical or radar data, in order to model forest carbon stocks and carbon uptake by land vegetation.

Huang et al. (2015) conducted a sensitivity analysis of multi – source SAR backscatter to changes in forest AGB, in order to investigate the influence of the incidence angle and soil moisture on SAR backscatter, the feasibility of cross – image normalization between multi-temporal and multi-sensor SAR data and the possibility of applying normalized backscatter data to detect forest biomass changes.

In a study conducted by Sandberg et al (2012), experimental P-band SAR data and reference data derived from laser scanning data were used for the development of regression models for biomass change estimation. Their results suggested that not only clear cuts, but also forest growth and thinning can be measured using P-band SAR backscatter.

A very interesting study, conducted by Suzuki et al (2013), investigates the potential of the P – band SAR system ALOS – PALSAR for estimating AGB and other biophysical parameters (tree height, DBG and tree stand density), in the boreal forest of Alaska. Their methodology is based on the backscatter intensity values (converted to σ^o) and *in situ* measurements. They conclude that a strong positive logarithmic correlation exists between the backscatter intensity and the forest AGB, with the correlation being stronger in the HV than in the HH polarization mode and finally they create a map of the geographical distribution of the forest AGB.

Morel et al. (2012) explored the potential of Landsat Enhanced Thematic Mapper (ETM+) imagery to quantify the expansion of planted oil palm area and changes in (AGB) in plantation and forest in Saba, Malaysian Borneo. With the combined use of ALOS PALSAR data, they studied the land cover change and the consequent carbon loss (release), due to forest conversion to oil palm. Finally, they came to estimate the

amount of carbon equivalent that were released. Their results, were presented as relevant for on-going efforts for the remote monitoring of carbon emission implications of forest loss as part of the United Nations Framework Convention on Climate Change's (UNFCCC's) proposed mechanism, Reduced Emissions from Deforestation and Degradation (REDD).

Lucas et al. (2010) evaluated the relationship between L – band SAR backscatter, derived from JAXA's ALOS PALSAR and AGB, for woody vegetation in Australia. They resulted that PALSAR data acquired when surface moisture and rainfall are minimal allow better estimation of the AGB of woody vegetation and that retrieval algorithms ideally need to consider differences in surface moisture conditions and vegetation structure.

Chang and Shoshany (2016) investigated the potential of the synergic use of Sentinel – 1 and Sentinel – 2 data for the mapping of biomass of Mediterranean shrublands, by developing a fusion biomass model based on C – band SAR backscatter coefficient, NDVI and *in situ* measurements. Most of the Sentinel – 1 parameters showed very low relationships with the shrub biomass, except HV backscatter coefficient (σ^0) and therefore they used the HV σ^0 in order to develop a regression model for biomass estimation.

In their study, Mermoz et al. (2015) examine the relationship between L-band SAR backscatter and dense tropical forest biomass for a large range of biomass values using both theoretical and experimental approaches. As they repost, both approaches revealed that after reaching a maximum value, SAR backscatter correlates negatively with forest biomass. This phenomenon is interpreted as a signal attenuation from the forest canopy as the canopy becomes denser with increasing biomass.

3. Basic principles of Remote Sensing

The term Remote Sensing refers to the act of monitoring and collecting information for an object of indifferent nature or size, or a phenomenon, from a distance and without having immediate contact with it. However, it is mostly used to describe the science and the art of monitoring the Earth and other celestial objects, from great distances, with the use of modern and high technology tools. It may refer to the monitoring of various states of matter (solids, liquids, gasses), or magnetic field, or radiation. The term usually refers to satellite remote sensing, but it can also refer to aerial photography or airborne systems, that might be equipped with various kinds of sensors or sophisticated cameras.

3.1. Electromagnetic radiation and electromagnetic spectrum

The electromagnetic (EM) spectrum is the range of all types of EM radiation.[1] EM radiation, in classical physics, is the flow of energy at the universal speed of light through free space or through a material medium in the form of the electric and magnetic fields that make up electromagnetic waves such as radio waves, visible light, and gamma rays[2].

Electromagnetic radiation can be described in terms of a stream of mass-less particles, called photons, each traveling in a wave-like pattern at the speed of light, while each photon contains a certain amount of energy.[3] The different types of radiation are defined by the amount of energy found in the photons. Radio waves have photons with low energies, microwave photons have a little more energy than radio waves, infrared photons have still more, then visible, ultraviolet, X-rays, and, the most energetic of all, gamma-rays.

[1] https://imagine.gsfc.nasa.gov/science/toolbox/emspectrum1.html
[2] https://www.britannica.com/science/electromagnetic-radiation

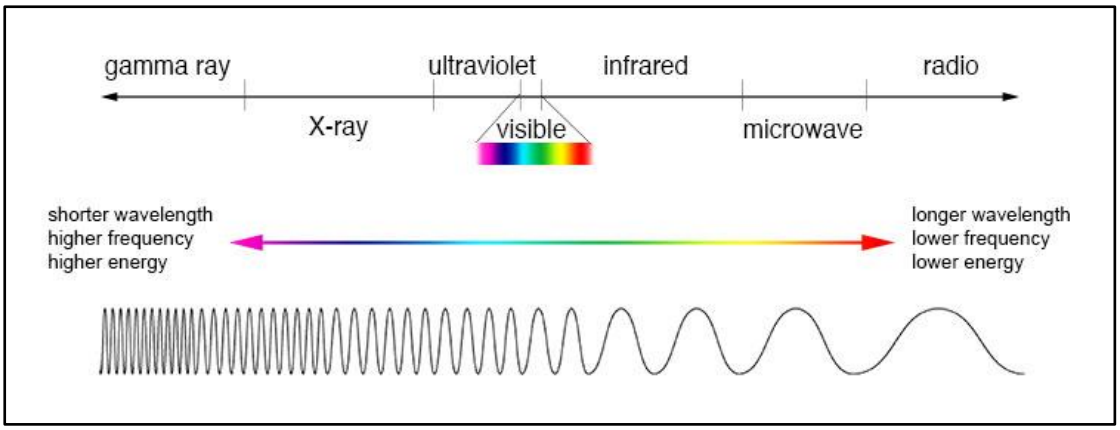

Figure 1. Comparison of wavelength, frequency and energy for the electromagnetic spectrum. Source:NASA.

Satellite remote sensing uses the electromagnetic spectrum in order to detect objects and phenomena and collect information about them, based on the interaction between electromagnetic radiation and their physicochemical properties or structural characteristics.

3.2. Different types of Earth Observation satellite systems

Satellite sensor types are roughly divided into two categories: active sensors and passive sensors.

Passive sensors

Remote sensors, which detect and record the natural (solar) radiation, are called passive sensors. Those systems, record the reflected solar radiation during the day, while they have the capacity to record the emitted thermal radiation, regardless of the presence of light, given that the amount of energy is high enough to be recorded.

Active sensors

Remote sensors, which record the electromagnetic waves that are emitted from an external source or the satellite system itself, are called active sensors. Usually, the

satellite or airborne system emits energy to the surface and subsequently, it records the signal's "echo" that is reflected by the surface and returns to the system.

According to NASA's EOSDIS, these are the types of active and passive sensors:

Active:

- Laser altimeter: An instrument that uses a lidar sensor, in order to measure the height of the instrument's platform above the surface. The height of the platform with respect to the mean Earth's surface is used to determine the topography of the underlying surface.

- Lidar: A light detection and ranging sensor that uses a laser (light amplification by stimulated emission of radiation) radar to transmit a light pulse and a receiver with sensitive detectors to measure the backscattered or reflected light. Distance to the object is determined by recording the time between transmitted and backscattered pulses and by using the speed of light to calculate the distance traveled.

- Radar—An active radio detection and ranging sensor that provides its own source of electromagnetic energy. An active radar sensor, whether airborne or spaceborne, emits microwave radiation in a series of pulses from an antenna. When the energy reaches the target, some of the energy is reflected back toward the sensor. This backscattered microwave radiation is detected, measured, and timed. The time required for the energy to travel to the target and return back to the sensor determines the distance or range to the target. By recording the range and magnitude of the energy reflected from all targets as the system passes by, a two-dimensional image of the surface can be produced.

- Ranging Instrument—A device that measures the distance between the instrument and a target object. Radars and altimeters work by determining the time a transmitted pulse (microwaves or light) takes to reflect from a target and return to the instrument. Another technique employs identical microwave instruments on a pair of platforms. Signals are transmitted from each instrument to the other, with the distance between the two determined from the difference between the received signal phase and transmitted (reference)

phase. These are examples of active techniques. An active technique views the target from either end of a baseline of known length. The change in apparent view direction (parallax) is related to the absolute distance between the instrument and target.

- Scatterometer—A high-frequency microwave radar designed specifically to measure backscattered radiation. Over ocean surfaces, measurements of backscattered radiation in the microwave spectral region can be used to derive maps of surface wind speed and direction.

- Sounder—An instrument that measures vertical distribution of precipitation and other atmospheric characteristics such as temperature, humidity, and cloud composition.

Passive:

- Accelerometer—An instrument that measures acceleration (change in velocity per unit time). There are two general types of accelerometers. One measures translational accelerations (changes in linear motions in one or more dimensions), and the other measures angular accelerations (changes in rotation rate per unit time).

- Hyperspectral radiometer—An advanced multispectral sensor that detects hundreds of very narrow spectral bands throughout the visible, near-infrared, and mid-infrared portions of the electromagnetic spectrum. This sensor's very high spectral resolution facilitates fine discrimination between different targets based on their spectral response in each of the narrow bands.

- Imaging radiometer—A radiometer that has a scanning capability to provide a two-dimensional array of pixels from which an image may be produced. Scanning can be performed mechanically or electronically by using an array of detectors.

- Radiometer—An instrument that quantitatively measures the intensity of electromagnetic radiation in some bands within the spectrum. Usually, a radiometer is further identified by the portion of the spectrum it covers; for example, visible, infrared, or microwave.

- Sounder—An instrument that measures vertical distributions of atmospheric parameters such as temperature, pressure, and composition from multispectral information.

- Spectrometer—A device that is designed to detect, measure, and analyze the spectral content of incident electromagnetic radiation. Conventional imaging spectrometers use gratings or prisms to disperse the radiation for spectral discrimination.

- Spectroradiometer—A radiometer that measures the intensity of radiation in multiple wavelength bands (i.e., multispectral). Many times the bands are of high-spectral resolution, designed for remotely sensing specific geophysical parameters[4]

3.2.1. SAR systems

Radar sensors operate in the microwave part of the electromagnetic spectrum. Wavelengths in this domain of the spectrum are a few centimeters long, 100,00o times longer than those in the visible region of the EM spectrum. Different radar sensors operate in different frequencies where, the longer the wavelength, the more effective their ability to penetrate a dielectric material (Ferretti, 2014). Due to their penetrative operating nature, radar systems are able to operate under any weather conditions, as they can penetrate clouds, fog and dust. SAR (Synthetic Aperture Radar) systems are active sensors, which means that instead of using the electromagnetic radiation from the sun, they produce their own electromagnetic radiation, through an antenna that is located on the satellite system or the spacecraft. The antenna emits microwave radiation pulses that last a few minutes, and then the "echoes" of these pulses that are recorded by the radar sensor. As a result, SAR sensors are independent of natural daylight, as they can operate day or night while penetrating through haze, smoke, and clouds (Goetz et al., 2009). Their ability to function independently of sun illumination and to generate images, no matter what the weather conditions are, have made satellite radar platforms an invaluable tool for

[4] https://earthdata.nasa.gov/user-resources/remote-sensors

earth observation and remote sensing, complementing the information gathered by optical sensors (Ferretti, 2014). It is important to be mentioned that this is particularly useful for monitoring areas prone to long periods of darkness – such as the Arctic – or providing imagery for emergency response during extreme weather conditions.[5] What is more, radars, are coherent sensors· that means that they can record both amplitude and phase information, for each ground target (Ferretti, 2014).

SAR vegetation applications

The sensitivity of SAR backscatter to both surface and volumetric properties provides an opportunity to estimate and monitor vegetation structure and dynamics over large areas (Svoray et al., 2001). Interaction of synthetic aperture radar (SAR) with vegetation is volumetric in nature; hence SAR is sensitive to the variation in vegetation density (Patel et al., 2006). For the purposes of this study, the information that is being used is the SAR backscatter, converted into backscatter coefficient (sigma^0), as this parameter has been found to present a strong relationship with forest biomass in several studies (e.g. Lei at al., 2008, Mitchard et al.2009, Sandberg et al., 2012, Huang et al., 2015). Backscatter is the portion of the outgoing radar signal that the target redirects directly back towards the radar antenna. Backscattering is the process by which backscatter is formed. The scattering cross section in the direction toward the radar is called the backscattering cross section; the usual notation is the symbol sigma (σ). It is a measure of the reflective strength of a radar target. The normalized measure of the radar return from a distributed target is called the backscatter coefficient, or sigma nought (σ^0), and is defined as per unit area on the ground. If the signal formed by backscatter is undesired, it is called clutter. Other portions of the incident radar energy may be reflected and scattered away from the radar or absorbed.[6]

Radar backscatter is a parameter that depends on the target's structural characteristics. Different surface features exhibit different scattering characteristics· urban areas return very strong backscatter, forests intermediate backscatter, calm water (smooth surface) low backscatter and rough sea increased backscatter due to wind and current effects. The radar backscattering coefficient σ^0 provides information

[5] http://www.esa.int/Our_Activities/Observing_the_Earth/Copernicus/Sentinel-1/Instrument
[6] https://earth.esa.int/handbooks/asar/CNTR5-2.html

about the imaged surface. It is a function of radar observation parameters (frequency f, polarisation p and incidence angle of the electromagnetic waves emitted), surface parameters (roughness, geometric shape and dielectric properties of the target).[7]

The amount of SAR signal that is attenuated due to vegetation volume depends on the frequency of operation, the polarization of the transmitted and received signal and the angle of incidence. Therefore, at a given angle of incidence, the frequency and polarization of the SAR signal are the most important sensor parameters that affect the backscatter from the canopy of a plant (Patel et al., 2006).

One of the major parameters that affect radar backscatter is frequency. The frequency of the incident radiation determines the penetration depth of the waves for the target imaged.[8]

Frequency band	**Frequency range (GHz)**	**Wavelength range (cm)**
P	0.255 – 0.390	133 – 76.9
L	0.390 – 1.550	76.9 – 19.3
S	1.550 – 4.20	19.3 – 7.1
C	4.20 – 5.75	7.1 – 5.2
X	5.75 – 10.90	5.2 – 2.7
K	10.90 – 36.0	2.7 – 0.83
K_u	10.90 – 22.0	2.7 – 1.36
K_a	22.0 – 36.0	1.36 – 0.83
Q	36.0 – 46.0	0.83 – 0.65
V	46.0 – 56.0	0.65 – 0.53
W	56.0 – 100.0	0.53 – 0.30

[7] https://earth.esa.int/web/guest/missions/esa-operational-eo-missions/ers/instruments/sar/applications/radar-courses/content-2/-/asset_publisher/qIBc6NYRXfnG/content/radar-course-2-parameters-affecting-radar-backscatter
[8] https://earth.esa.int/web/guest/missions/esa-operational-eo-missions/ers/instruments/sar/applications/radar-courses/content-2/-/asset_publisher/qIBc6NYRXfnG/content/radar-course-2-parameters-affecting-radar-backscatter

Table 1. Εικόνα 1 Radar frequency bands and corresponding wavelengths.

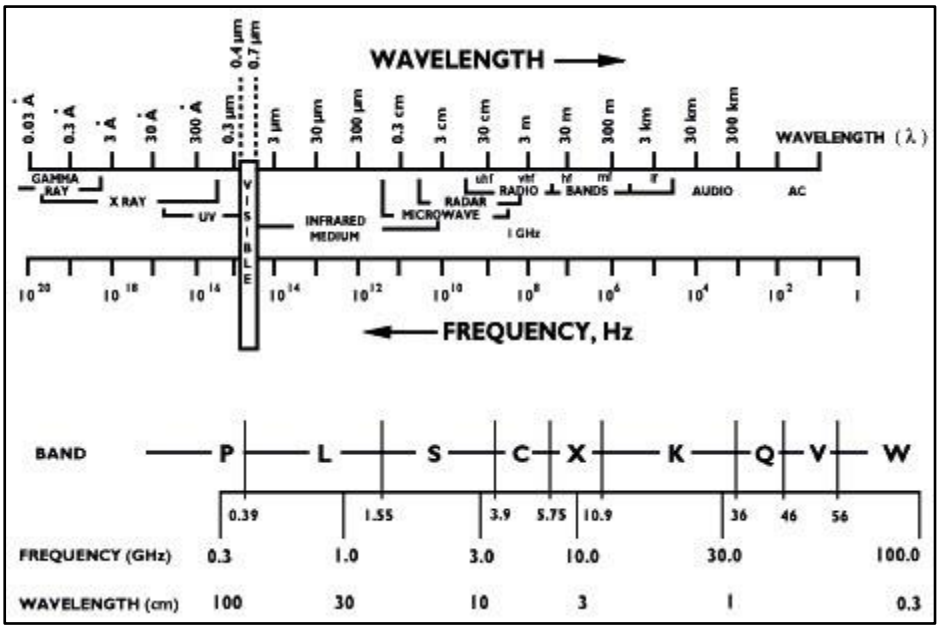

Figure 2. Radar wavelengths and frequencies. Source: ESA.

Dobson et al. (1992) observed that the depth of penetration of a signal into a forest canopy is governed by the degree of interaction that the field has with the canopy; C and X band microwave frequencies (5 and 3cm wavelengths) interact more strongly with the leaves and branches of the upper canopy while P and L band signals (68 and 24cm wavelength) penetrate through the upper canopy of the forest (Patel et al., 2006).

Another parameter that has to be taken into account is microwave polarization. The microwave polarization refers to the orientation of the electric field vector of the transmitted beam with respect to the horizontal direction; if the electric field vector oscillates along a direction parallel to the horizontal direction, the beam is said to be "H" polarized, while on the other hand, if the electric field vector oscillates along a direction perpendicular to the horizontal direction, the beam is "V" polarized.[9] A polarimetric radar can be designed to operate as a single-pol system, where the there is a single polarization transmitted and a single polarization received. A typical single-pol system would transmit horizontally or vertically polarized waveforms and

[9] https://crisp.nus.edu.sg/~research/tutorial/freqpol.htm

receive the same (giving HH or VV imagery), while a dual-pol system might transmit a horizontally or vertically polarized waveform and measure signals in both polarizations in receive (resulting in HH and HV imagery). A quad-pol or full-pol system would alternate between transmitting H-and V-polarized waveforms and receive both H and V (giving HH, HV, VH, VV imagery).[10]

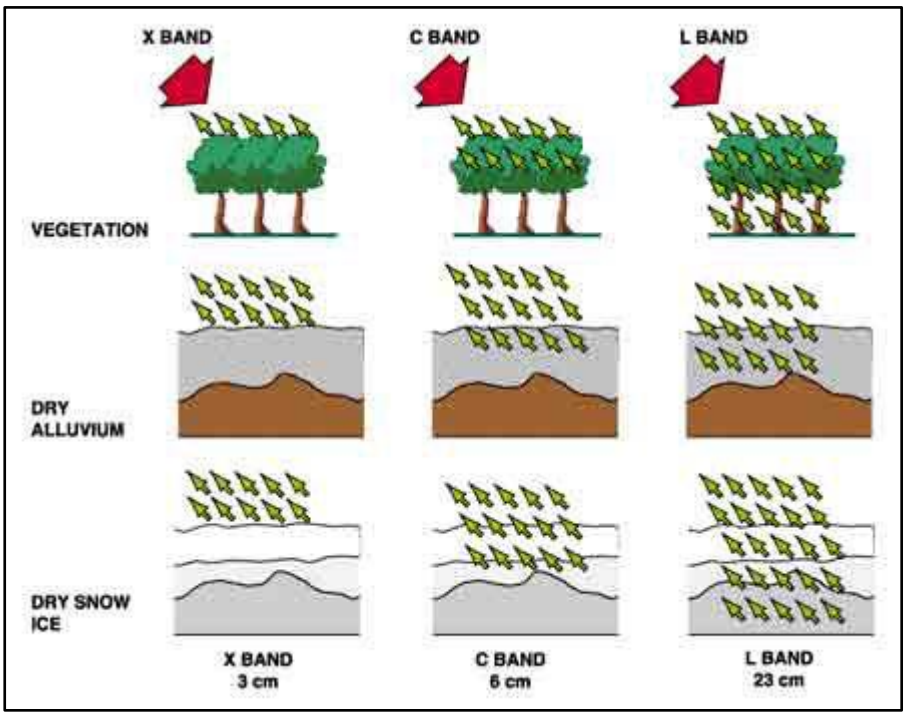

Figure 3. Source: interaction of SAR backscatter of different bands with surfaces. Source: ESA

[10] https://nisar.jpl.nasa.gov/technology/polsar/#

3.2.2. Sentinel – 1

A new family of space missions for Earth Observation, called Sentinels, is being developed by ESA, for the operational needs of the Copernicus programme. Each Sentinel mission is based on a constellation of two satellites to fulfil revisit and coverage requirements, providing robust datasets for Copernicus Services. [11]

Copernicus is a European Union Programme aimed at developing European information services based on satellite Earth Observation and *in situ* (non-space) data. This initiative is headed by the European Commission (EC) in partnership with the European Space Agency (ESA) and the European Environment Agency (EEA).

Sentinel-1 is a polar-orbiting, all-weather, day-and-night radar imaging mission for land and ocean services. Sentinel-1A was launched on 3 April 2014 and Sentinel-1B on 25 April 2016. Both were taken into orbit on a Soyuz rocket from Europe's Spaceport in French Guiana.[12] The identical satellites orbit Earth 180° apart and at an altitude of almost 700 km. This configuration optimizes coverage, offering a global revisit time of just six days. At the equator, however, the repeat frequency is just three days and less than one day over the Arctic. Europe, Canada and main shipping routes are covered in less than three days.[13]

The radar operates in two main modes: Interferometric Wide swath (IW) and Wave. There's also the potential for operating it in two additional modes: Stripmap and Extra Wide Swath. For the purposes of the current study, the IW mode has been used. Interferometric Wide swath mode, the default mode over land, has a swath width of 250 km and a ground resolution of 5 x 20 m. This mode images in three sub-swaths, using the Terrain Observation with Progressive Scans SAR – or TOPSAR. With this technique, the radar beam scans back and forth three times within a single swath (called sub-swaths), resulting in a higher quality and homogeneous image throughout the swath.[14] All modes can be operated in several polarization schemes.

[11] http://www.esa.int/Our_Activities/Observing_the_Earth/Copernicus/Overview4
[12] http://www.esa.int/Our_Activities/Observing_the_Earth/Copernicus/Overview4
[13]http://www.esa.int/Our_Activities/Observing_the_Earth/Copernicus/Sentinel-1/Satellite_constellation
[14] http://www.esa.int/Our_Activities/Observing_the_Earth/Copernicus/Sentinel-1/Instrument

IW mode features both single (HH or VV) and dual polarization (VV+VH or HH+HV). [15]

[15] http://www.esa.int/Our_Activities/Observing_the_Earth/Copernicus/Sentinel-1/Data_products

4. The forests as carbon sinks and biogeochemical cycles of carbon

The term "biogeochemical cycles" is generally used to describe the circulation of chemical elements within the global ecosystem, through different kinds of fluxes. To put it more precisely, according to Hedges (1992), biogeochemical cycles are the biological, geological and chemical processes by which materials and energy are exchanged and reused at the land – atmosphere – ocean system. These intermeshed processes operate on time- scales of microseconds to eons and occur within domains that range in size from a living cell to the entire global ecosystem (atmosphere-ocean system) (Hedges, 1992).

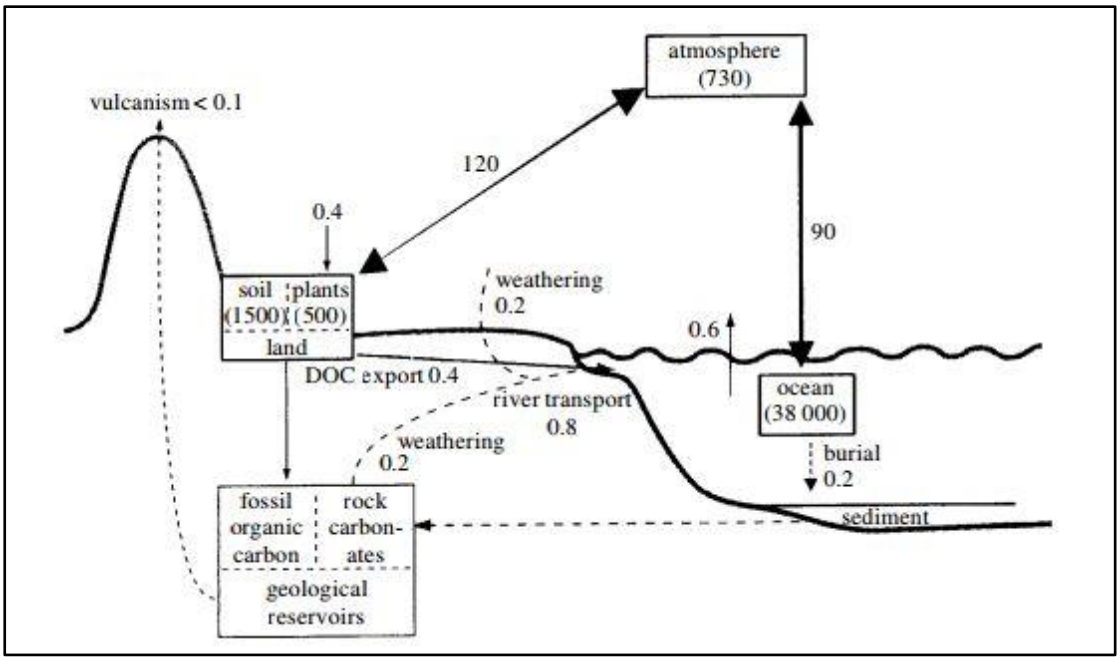

Figure 4. Main components of the carbon cycle. The thick arrows represent gross primary production and respiration by the biosphere and physical sea{air exchange. The thin arrows denote natural fluxes which are important over longer time-scales. Dashed lines represent fluxes of carbon as calcium carbonate. The units for all fluxes are PgC yr^{-1}; the units for all compartments are PgC. Source: Malhi et al. (2002)

The global carbon cycle can be viewed as a series of reservoirs of carbon in the Earth System, which are connected by exchange fluxes of carbon (Ciais et al, 2013). The storage of carbon on land is partitioned between soil and vegetation; globally, soils contain more than 75% of all terrestrial carbon stocks, although their

contribution to the total varies with latitude and land use (Swingland, 2013). Forests and wooded grasslands/savannahs are by far the biggest carbon storehouses, respectively accounting for 47% and 25% of the global total, while other ecosystems tend to maintain comparatively little aboveground carbon, with the stock in soil varying between 100 and 225 PgC (Malhi et al. 2013).

Between 30% and 50% of the total amount of carbon absorbed by vegetation (gross primary production (GPP)) is used to support plant metabolic processes and is released back to the atmosphere as a by-product of respiration (Amthor & Baldocchi 2001). The remaining carbon is fixed as organic matter above or below the ground and is termed net primary production (NPP), which varies depending on the vegetation type, according to climate, soil type and species composition. (Malhi et al., 2002).

5. Carbon monitoring

5.1. The importance of monitoring forest carbon stocks

Implementing effective GHG management strategies in order to safeguard climate, requires full knowledge of the natural carbon cycle; today, only about half of the CO_2 emitted from fossil fuels remains in the atmosphere, but little we know about whether or to what extent this fraction is changing, nor do we understand the forces driving global and regional changes to land and ocean carbon uptake and release (Ciais et al., 2010). Individual nations may implement emission controls, but a comprehensive strategy of emission offset and natural sink conservation must be designed to effectively curve down the increase of CO_2 concentrations in the future and verify that in an independent transparent manner (Ciais et al., 2010). Carbon monitoring during time is an essential practice in order for the scientific community to be aware of both the status and the dynamics of the carbon equilibrium on regional and global scales. Furthermore, the development of a global time series of data regarding the status of the terrestrial carbon stocks is essential in order for the scientific community and the future generations to be able to shape an integrated and in – depth knowledge on the subject and to model and predict the future responses of the ecosystems regarding the carbon equilibrium, based on specific climatic scenarios and scenarios regarding carbon emissions. In the same rationale, carbon monitoring can also play the role of a regulating mechanism; international organizations such as the IPCC and the UNFCCC need this knowledge in order to force governmental bodies to adapt to the requirements regarding environmental sustainability, by adopting environmentally friendly policies and practices, controlling/ reversing land degradation, reducing carbon emissions and increase or maintain forest carbon stocks.

Satellite derived data and remote sensing techniques constitute a great tool for carbon monitoring. However, carbon estimation methods and data are always based on *in-situ* measurements, as terrestrial carbon cannot be directly estimated by the use of electromagnetic radiation. As carbon monitoring depends on biomass estimation and given the fact that biomass values varies a lot, depending on the species and on a plethora of characteristics of the land, carbon estimation models need to be calibrated with region – specific *in situ* measurements. Despite the fact that carbon estimations

by means of remote sensing are based on ground truth data, direct measurements of biomass in the field, could never be considered sufficient for carbon monitoring on a global scale, without the combined use of satellite remote sensing, as they are costly and time consuming and as such they lack the spatial and temporal continuity that is needed for the integrated approach of the subject. In defense of the abovementioned statement, it is important to emphasize that the recommendation of the IPCC, with respect to the UNFCCC's REDD+ mechanism, is the combined use of Earth Observation (EO) data and field-based inventory, for the estimation of forest area, carbon stocks and changes (Mitchell et al., 2017).

5.2. *In situ* measurements and allometrcic equations

Carbon monitoring with the use of satellite sensors is generally based on *in situ* measurements, for the most part. At regional and national scales, forest inventory data – based biomass models are widely used as a tool for biomass assessment (Cheng et al., 2014). Long-term forest inventories are extremely useful in order to evaluate the magnitude of carbon fluxes between aboveground forest ecosystems and the atmosphere (Chave et al., 2005). *In situ* forest data constitute the foundation for each and every biomass estimation method available. Even the use of the most accurate technological tools for biomass estimation, requires at least ground truth data for validation and calibrations purposes.

As forest biomass differs significantly between different types of ecosystems, the development of big collections of allometric equations, for different types of ecosystems is of great importance. The term "allometry", in its broadest sense, designates the differences in proportions correlated with changes in absolute magnitude of the total organism or of the specific parts under consideration (Gould et al., 1966). If we consider trees on a population scale, we can see that the different dimensions of an individual are statistically related with one another; this relation stems from the ontogenic development of individuals which is the same for all, within life history related variability (Picard et al., 2012). For instance, the proportions between height and diameter, between crown height and diameter or between biomass and diameter follow rules that are the same for all trees, big or small, as long as they are growing under the same conditions; this is the basic principle of

allometry and it can be used to predict a tree variable (typically its biomass) from another dimension (e.g. its diameter) (Picard et al., 2012). An allometric equation is a formula that quantitatively formalizes this relationship. The allometric equations used to predict the biomass of a tree from "easier-to-measure" dendrometric characteristics, such as tree diameter or height, are key factors in estimating the contribution made by forest ecosystems to the carbon cycle (Picard et al., 2012).

5.3. Satellite vegetation applications and modern perspectives

As referred by the Global Observation of Forest and Land Cover Dynamics (GOFS – GOLD) panel of the Global Terrestrial Observing System (GTOS), the sustainable development of forests has emerged as one of the most difficult, serious, and pressing environmental issues of our time, as human-induced changes in Earth's forests have affected natural resource availability, biodiversity, atmospheric composition, and climate[16] . Knowledge on both the state and the dynamics of land vegetation is a key parameter, in order for the governmental bodies and the international/ intergovernmental organizations (e.g. IPCC), the scientific community and the humanity to protect the Earth's natural resources, to obtain and maintain balance and to mitigate the human induced factors associated with climate change, land degradation and environmental insecurity.

In situ measurements have been always serving the needs of the scientific community in data, constituting one major source of knowledge, regarding environmental issues. Their advantages lie in their accuracy and precision, however, they lack the spatial and temporal extent, as they are costly and can even have, in some cases, destructive effects for the ecosystem. What is more, a big part of the planet constitutes of areas rather inaccessible. Those gaps and discontinuities in data can be overcome with the use of satellite sensors, that provide information globally and in a fairly good temporal extent. Therefore, it becomes clear, that the monitoring of land vegetation, by means of remote sensing is a fundamental tool for the integrated approach of the subject.

[16] http://www.fao.org/gtos/gofc-gold/overview.html

During the last decades, a great amount of methods have been developed, regarding remote sensing vegetation applications, with the use of optical, radar and lidar data. Several methodologies have already been presented through published studies, as referred in the literature review. It is important to this point to make a reference on the future mission of the European Space Agency, the "Biomass" mission, which aims to provide global maps of the amount of carbon stored in the world's forests and how this changes over time, mainly through absorbing carbon dioxide, which is released from burning fossil fuels. As stated by the ESA, although forest type and forest cover worldwide can be detected by today's satellites, Biomass mission will take the information to the next level; due for launch in 2021, the satellite will carry the first P-band synthetic aperture radar, able to deliver accurate maps of tropical, temperate and boreal forest biomass[17].

[17] https://earth.esa.int/web/guest/missions/esa-future-missions/biomass

6. Materials and methods

6.1. Data

6.1.1. In situ

For the purposes of this study, AGB was estimated with the use of *in situ* data. In particular, DBH and tree height were measured directly in the field, with the use of analogical forestry tools. These data refer to three sample plots, in the study area of Mount. Parnitha. More details on the methods used for the field measurements can be found in the methodology chapter. Furthermore, *in situ* biomass data for 5 sample plots, that correspond to 3 additional study sites (namely, Mount. Vardousia, Mount. Parnassos and Mount. Dirfi) were provided by courtesy of the Assistant Researcher of the Forest Research Institute (FRI), of the Hellenic Agricultural Organisation, Dr. Nikolaos M. Fyllas.

6.1.2. Satellite

Satellite data derived from the Sentinel – 1 satellite system were used for the purposes of the current study. Sentinel – 1 operates within the context of the Sentinel Missions, under the EU Copernicus programme for Earth Observation.

Products

Level-1 Ground Range Detected (Sentinel – 1 SAR)

Level – 1 Ground Range Detected (GRD) products consist of focused SAR data that has been detected, multi-looked and projected to ground range using an Earth ellipsoid model. Phase information is lost. The resulting product has approximately square resolution pixels and square pixel spacing with reduced speckle at the cost of reduced geometric resolution.[18]

[18] https://sentinel.esa.int/web/sentinel/missions/sentinel-1/data-products

For the purposes of this study, the High Resolution GRD product was used, in Interferometric Wide Swath (IW) mode. The Interferometric Wide swath mode is the main acquisition mode over land and satisfies the majority of service requirements. It acquires data with a 250 km swath at 5 m by 20 m spatial resolution (single look). IW mode captures three sub-swaths using Terrain Observation with Progressive Scans SAR (TOPSAR). With the TOPSAR technique, in addition to steering the beam in range as in ScanSAR, the beam is also electronically steered from backward to forward in the azimuth direction for each burst, avoiding scalloping and resulting in homogeneous image quality throughout the swath.

Azimuth resolution is reduced compared to SM due to the shorter target illumination time of the burst. Using the sweeping azimuth pattern, each target is seen under the same antenna pattern, independently from its azimuth position in the burst image. By shrinking the azimuth antenna pattern, as seen by a target on the ground, scalloping effects on the image can be reduced. Bursts are synchronised from pass to pass to ensure the alignment of interferometric pairs.

TOPSAR mode is intended to replace the conventional ScanSAR mode, achieving the same coverage and resolution as ScanSAR, but with a nearly uniform SNR (Signal-to-Noise Ratio) and DTAR (Distributed Target Ambiguity Ratio).[19]

As soil moisture has an impact on the backscatter signal of SAR sensors, it should be noted here that no precipitation events had occurred during the last 20 days before the sensing date of the 2 GRD products that were used. However, the sensor is a C-band, which means that information is largely derived from the canopy.

6.2. Study sites

Mount. Parnitha

Mt. Parnitha National Park is one of the ten sites that have been characterized as national parks in Greece, and is located in Attica, very close to the metropolitan city of Athens (35 km northbound) (Ganatsas et al, 2012). In 1961 the entire mountain

[19]https://sentinel.esa.int/web/sentinel/user-guides/sentinel-1-sar/acquisition-modes/interferometric-wide-swath

(~25,000 hectares) was declared a National Park and it is of great importance for the wider Athens metropolitan area (Efthimiou et al., 2014). The geological substrates of Mt. Parnitha are schists (which appear in the valleys) and limestone (which appear on the tops), and some flysch, while the climate of the mountain is substantially different from the climate of the rest of the Attica area, especially with regard to air temperature and precipitation (Efthimiou et al., 2014). Tectonically, the mountain range lies between two Quaternary rift systems in central Greece: the Gulf of Corinth Rift and the Gulf of Evia rift (Ganas et al., 2004). Parnitha's wild vascular flora comprises 1096 taxa, belonging to 90 families (Aplada et al., 2007). The study area concerns the region of the conifer species *Abies Cephalonica* Loudon, 1838 (Greek fir), which is described in the next sub-chapter.

	Latitude	Longitude	Plot dimensions
Plot 1.	38°10'37.34"N	23°43'50.09"E	Approx. 25m x 25m
Plot 2.	38°10'17.00"N	23°43'30.79"E	Approx. 25m x25m
Plot 3.	38°10'3.47"N	23°44'0.96"E	Approx. 33m x 33m

Table 2. Sample plots: center coordinates, elevation and dimensions.

Figure 5. Indicative locations of the 4 study sites. Source: Google Earth.

In summer 2007, a catastrophic fire burned down 18,957 ha (Fig. 2) of the *A. cephalonica* forest, 10,562 ha of *Pinus halepensis*, and 3,976 ha of evergreen broad-leaved shrublands (Ganatsas et al, 2012). Since then continuous efforts take place in order to reestablish and restore the forest in the burned area. (Efthimiou et al., 2014).

Mount. Parnassos

The National Park of Parnassos was established in 1938 and is the second Greek National Park -the first being Mount Olympos[20]. Parnassos is a complex ecosystem that consists of a wide variety of landscapes and habitats, resulting to rich and rare biodiversity. The geological substrate consists mainly of hard limestone that forms karst landforms. The protected part of the mountain is characterized by a large number of special scientific importance and significance plant taxa. In particular, 854 taxa have been reported, 6 of which are endemic, while, a large number are stenoendemic (endemic to Central Greece, Greece etc). Several species in the area are assigned to different risk categories according to WCMC, P.D.67/1981, UNEP, RDB and the Berne Convention.[21] The area consists of the following vegetation zones:

- the non – forested zone of high mountains

- the beech - fir zone, including not only *A. cephalonica* forests, but *Pinus nigra* clusters as well

- the deciduous broadleaf zone, including deciduous forests as well as kermes oak brushlands

- the coastal, hill & sub-mountain zone is fragmented, limited to small spots, including broadleaved evergreen thickets of Oak and *Pistacia lentiscus* trees.

- the riparian ecosystems, appearing mostly along the river margins and banks. [22]

Mount. Dirfi (Steni forest)

The Steni forest is located at Evia island, the second largest Greek island, at a distance of 31 km from the prefecture capital Chalkida, and 120 Km from Athens, the capital of Greece and it includes a significant number of protected areas: one Aesthetic forest, 14 Wild Life Refugees, 3 Monuments of Nature, 6 areas in the NATURA 2000 network and more than 28 large and small Wetlands (Efthimiou and Karageorgos, 2010). It is part of the Dirfi forest complex, covering a total area of 417 hectares (Fig. 1) and it extends from an altitude of 900m to 1147m

[20] Natura 2000 data form standard data form for special protection areas (SPA) for sites eligible for identification as sites of community importance (SCI) and for special areas of conservation (SAC).
[21] http://en.parnassosnp.gr/general-info.aspx
[22] http://en.parnassosnp.gr/vegetation-zones.aspx

(Efthimiou and Karageorgos, 2010). The site gains special ecological and aesthetic interest from the combination of its floristic diversity with the geomorphological and hydrological features. In this area, there exist many representative habitat types, which support numerous local endemic or greek endemic plant species. [23] Geologically, the area consists of slates and phyllites that are evolving to crystallic limestones, while the climate is temperate Mediterranean, with warm summers and mild to heavy winters, with large dry period from April to October (Efthimiou and Karageorgos, 2010).

Mount. Vardousia

Mount. Vardousia constitutes the southernmost part of Pindus mountain range. It is one of the few mountains in Greece having Alpine characteristics, while more than ten peaks exceed 2000 meters altitude and its expanse is 30 kilometers from north to south and 15 kilometers from west to east (Karamihalaki et al., 2015). Part of the area is included in the Natura 2000 network of protected areas, with the location name "Ori Vardousia" and under the code GR2450001. The occurrence of a great number of endemic and rare plants, especially in the extraforestial plant associations, renders the area as an important one from an ecological point of view, according to Natura 2000.

6.2.1. Studied Species

The genus *Abies* consists of about 40 evergreen species, found in the Northern Hemisphere (Raftoyannis et al., 2008). The Mediterranean Basin hosts eight *Abies* taxa and constitutes one of the genus distribution centers; among those, the endemic to Greece *A. cephalonica* is the only Mediterranean taxon with island populations, in Euboea and Cephalonia, in the Aegean and the Ionian Sea, respectively (Politi et al., 2011). *A. cephalonica* is endemic to the mountains of central and southern Greece and indigenous to islands of Cephalonia (Ionian Sea), Euboea in the Aegean Sea, Sterea Hellas, and in the far south of Peloponnesos (Jagodzinski et al., 2011). The species can be found on a variety of

[23] https://filotis.itia.ntua.gr/biotopes/c/GR2420002/

bedrocks, including gneiss, serpentine, flysch, schist, limestone and dolomite, without showing any preference on a specific soil type (Samaras, 2012). Greek firs reach 30-35 m of height and 1.5-2 m of diameter at breast height (Jagodziński et al, 2011). The natural altitudinal distribution of Greek fir ranges from 400 m to 2300 m a.s.l (Samaras, 2012).

6.3. Methodology

6.3.1. *In situ* Above Ground Biomass estimation

For the purposes of the current study, AGB was estimated via *in situ* measurements that took place in three different sites of the *A. cephalonica* zone of the forest ecosystem of Mount. Parntitha. The three plots were of about 750 – 1000 m^2 each (table) and every single live tree, with trunk diameter >4cm, which fall within each of the demarcated areas, was sampled. The measurements were conducted on three different days, during July 2017. Tree structural features (dbh and tree height) were measured directly in the field, with the use of analogical forestry tools; for the measurement of the dbh, a tree caliper (image 7) was used, while tree height was estimated with the use of a clinometer (image8).

Figure 6. Using a tree caliper for the measurement of DBH.

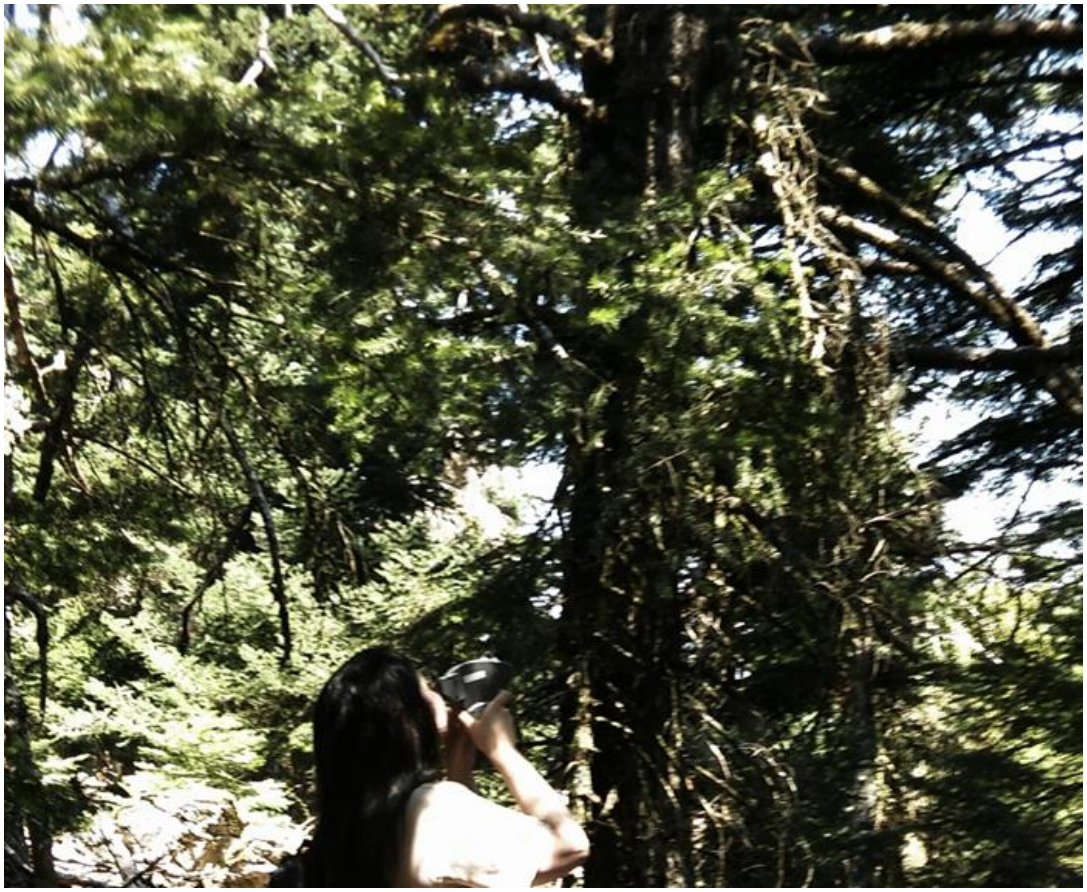

Figure 7. Using a clinometer for tree height estimation.

Subsequently, AGB was estimated in two ways, with the use of two different allometric equations. Since no allometric equations for biomass estimation were found through the literature for the species *A. cephalonica*, *Abies alba* biomass allometric equations were used, as this species was considered the most similar to the studied species, in terms of biomass estimation.

Figure 8. Picture taken inside one of the sample plots of the Parnitha study site, during field work.

Figure 9. Field work equipment, including measuring tape, tree caliper, clinometer, compass and notepad.

Allometric equation 1:

In the first instance, AGB was estimated with the use of the biomass allometric equation, developed by Gasparini et al. (2006), for the species *Abies alba*. According to this study, AGB can be estimated as follows:

$$W_{tot} = 3.3424 + 1.6487 * 10^{-2}d^2h + 8.1355 * 10^{-2}d^2 \quad (1)$$

where,

W_{tot} = total aboveground dry weight (total AGB) (kg)

d: diameter at breast height (cm)

h: tree height (m)

Allometric equation 2 (set of allometric equations):

Subsequently, AGB was cumulatively estimated, with the use of a set of allometric equations developed by Ruiz-Peinado et al. (2011). In their study, they suggest 3 individual allometric equations, for the estimation of (i) stem biomass, (ii) biomass of thick and medium branches and (iii) biomass of thin branches and needles. The sum of the abovementioned parameters was used for the estimation of the total AGB. The equations are provided below:

i) Stem:

$$W_s = 0.0189 * d^2*h \quad (2)$$

ii) Thick + Medium branches:

$$W_{b7} + W_{b27} = 0.0584 * d^2 \quad (3)$$

iii) Thin branches + needles:

$$W_{b2+n} = 0.0371 * d^2 + 0.968 * h \quad (4)$$

where,

W_s: Biomass weight of the stem fraction (kg). W_{b7}: Biomass weight of the thick branch fraction (diameter larger than 7 cm) (kg). W_{b2-7}: Biomass weight of medium branch fraction (diameter between 2 and 7 cm) (kg). W_{b2+n} Biomass weight of thin branch fraction (diameter

smaller than 2 cm) with needles (kg). W_r: Biomass weight of the belowground fraction (kg); d: dbh (cm). h: tree height (m).

Over and above the 3 plots that were sampled for the estimation of AGB in the forest ecosystem of Mount. Parnitha, AGB values for 5 additional sample plots, corresponding to 3 study sites (namely, Mount. Vardousia, Mount. Parnassos and Mount. Dirfi), were kindly provided by courtesy of the Assistant Researcher of the Forest Research Institute (FRI), of the Hellenic Agricultural Organisation, Dr. Nikolaos M. Fyllas.

In the interest of clarity, it has to be emphasized that field measurements conducted by different research teams may imply irregularities due to use of different measurement tools and different approaches to the same subject. What is more, AGB estimation results may differ on account of different allometric equations usage. As the data that were kindly provided by our colleagues from the FRI have not been published at the moment, further details on the exact methodology followed, the size of the plots and the allometric equations that were used, are about to become known through their upcoming publications. The provided AGB values were measured in Mg/ ha.

In order for all the plots to refer to the same spatial extent and be comparable among each other, AGB values were converted to Mg/ ha, for all the sample plots used in this study.

Conversion to carbon

According to the FC Woodland Carbon Code: *Carbon Assessment Protocol*, published by the Forestry Commission of Edinburgh (Jenkins et al., 2011), the conversion from biomass to carbon, is given by multiplying AGB by the factor 0.5.

The AGB values and the corresponding carbon amounts of the 3 sample plots, for the study area of Mount. Parnitha, are provided in table below.

Plots	AGB(1) (Mg/ha)	Carbon(1) (Mg/ha)	AGB(2) (Mg/ha)	Carbon(2) (Mg/ha)
Parnitha 1	102.960	51.480	121.130	60.565
Parnitha 2	94.810	47.405	103.380	51.69
Parnitha 3	107.580	53.790	127.110	63.555

Table 3. AGB and carbon per sample plot.

6.3.2. C – band SAR backscatter coefficient ($sigma_0$)

In this study, in order for the relationship between AGB and satellite derived SAR backscatter coefficient ($sigma_0$) to be explored, SAR backscatter $sigma_0$ values were extracted from Sentinel – 1 satellite data. For the retrieval of this information, the high resolution GRD product, in IW mode was used.

For the processing of the GRD products, the open source software SNAP was used. SNAP is a common architecture application platform, designed to host the ESA toolboxes for the processing and implementation of Earth Observation data.

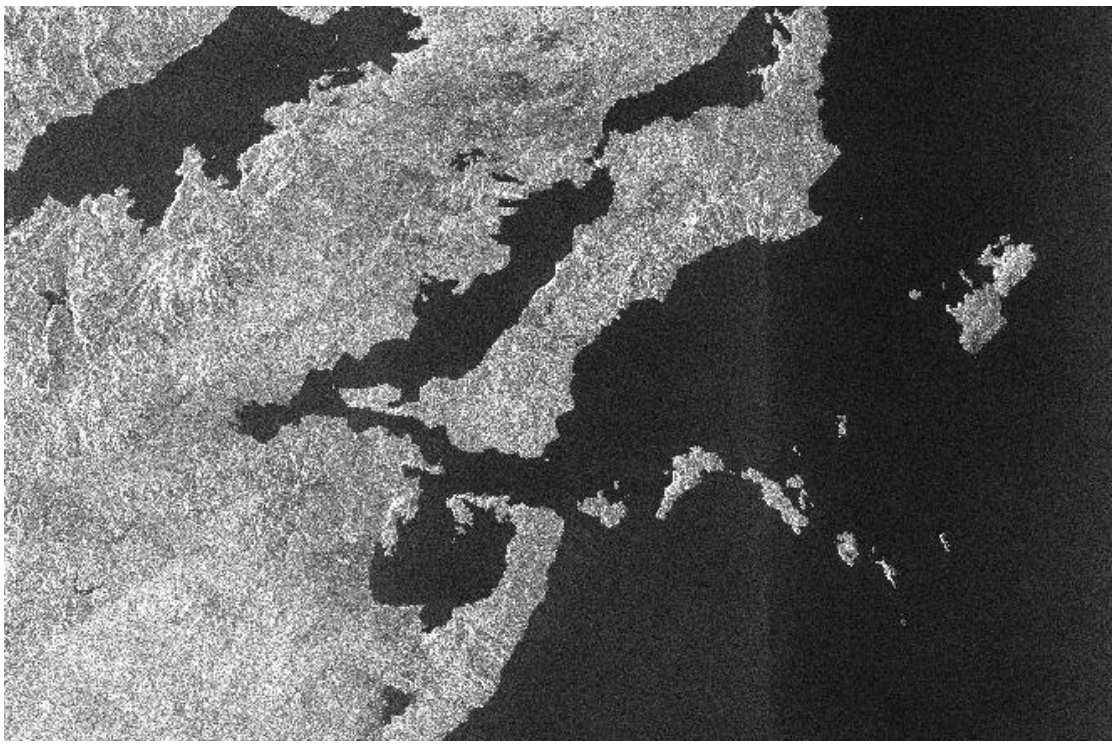

Figure 10. Initial satellite image. Level - 1 GRD high resolution product in IW mode. Pass: Ascending. Sensing date: 16/07/2017.

Figure 11. Initial satellite image. Level - 1 GRD high resolution product in IW mode. Pass: Descending. Sensing date: 16/07/2017.

For the processing of the satellite data and the retrieval of the SAR backscatter coefficient ($sigma_0$) values, the following steps were applied:

1. Orbit file

The orbit state vectors provided in the metadata of a SAR product are generally not accurate and can be refined with the precise orbit files which are available days-to-weeks after the generation of the product. The orbit file provides accurate satellite position and velocity information. Based on this information, the orbit state vectors in the abstract metadata of the product are updated.

2. Calibration to $sigma_0$

The objective of SAR calibration is to provide imagery in which the pixel values can be directly related to the radar backscatter of the scene. Though uncalibrated SAR imagery is sufficient for qualitative use, calibrated SAR images are essential to quantitative use of SAR data.

Typical SAR data processing, which produces level 1 images, does not include radiometric corrections and significant radiometric bias remains. Therefore, it is

necessary to apply the radiometric correction to SAR images so that the pixel values of the SAR images truly represent the radar backscatter of the reflecting surface. The radiometric correction is also necessary for the comparison of SAR images acquired with different sensors, or acquired from the same sensor but at different times, in different modes, or processed by different processors.

For converting digital pixel values to radiometrically calibrated backscatter, all the required information can be found in the product. A calibration vector is included as an annotation in the product allowing simple conversion of image intensity values into sigma or gamma nought values.

In order for the pixel values to be directly related to the radar backscatter of the scene, the application output scaling applied by the processor must be undone and the desired scaling must be applied. For the Sentinel – 1, level-1 products, four calibration Look Up Tables (LUTs) are provided, for the production of $ß^0_i$, σ^0_i and γ_i or the return to the Digital Number (DN). The LUTs apply a range-dependent gain including the absolute calibration constant. For GRD products, a constant offset is also applied.

The following equation is used in order for the radiometric calibration to be applied to the S – 1 products:

$$value(i) = \frac{|DN_i|^2}{A_i^2}$$

where, depending on the selected LUT,

value(i) = one of β^0_i, σ^0_i, or γ_i or original DN_i.

A_i = one of *betaNought* (*i*), *sigmaNought t*(*i*),

Bi-linear interpolation is used for any pixels that fall between points in the Look up Table (LUT).

Finally, $sigma_0$ values were converted to decibel (db).

3. Speckle filtering

SAR images have inherent salt and pepper like texturing called speckles, which degrade the quality of the image and make interpretation of features more difficult. Speckles are caused by random constructive and destructive interference of the de-phased, but coherent return waves scattered by the elementary scatters within each resolution cell.

The usage of filters for reduction of the speckle was attempted, in order to examine whether the backscatter coefficient values are affected and if so, in what manner. It appears that although the filters create smoother with reduced "salt and pepper", no difference is noticed in the (converted into db) backscatter sigma$_0$ values.

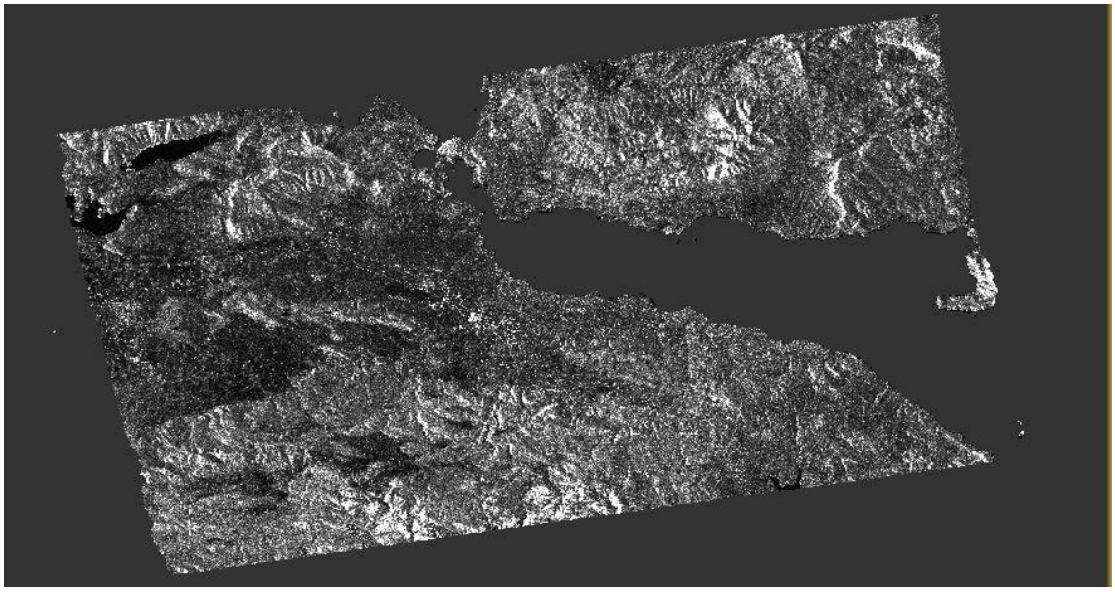

Figure 12. GRD product subset scene in IW mode (high resolution). Pass: ascending. No speckle filter applied.

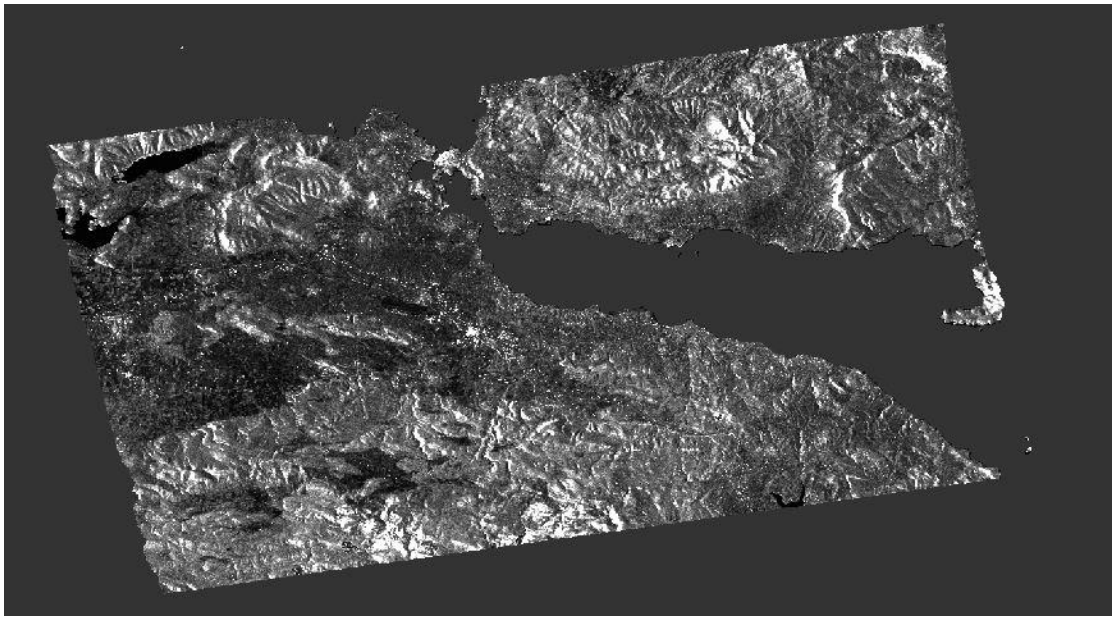

Figure 13. GRD product subset scene in IW mode (high resolution). Pass: ascending. "Lee sigma" speckle filter applied.

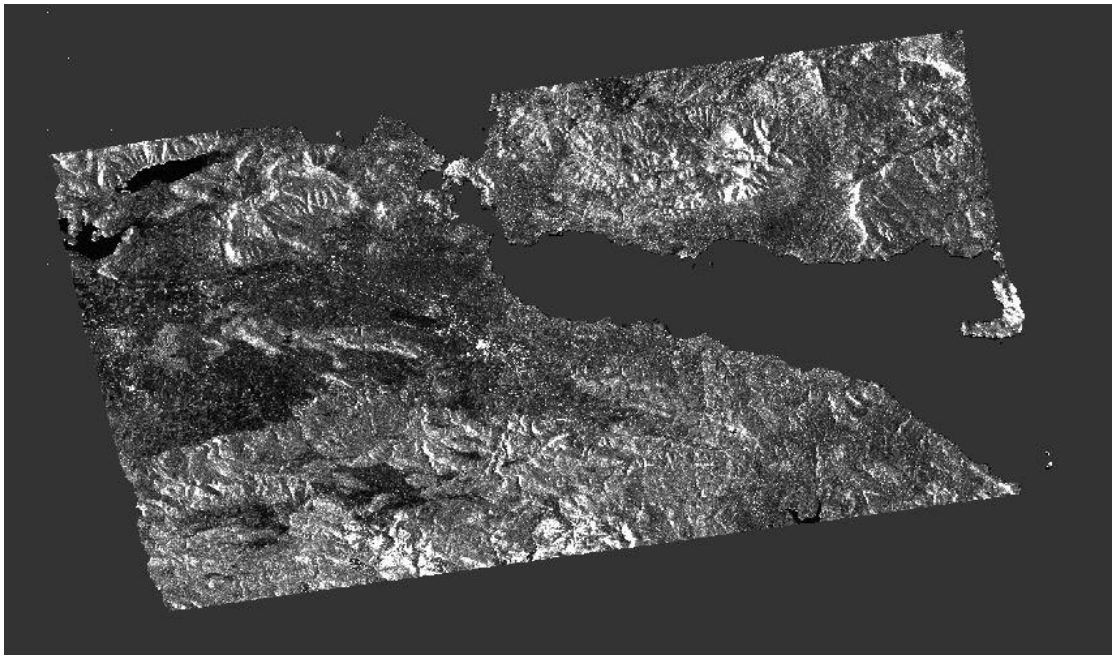

Εικόνα 2. GRD product subset scene in IW mode (high resolution). Pass: ascending. "Refined Lee" speckle filter applied

As the despeckled images showed no significant differentiations regarding the backscatter coefficient values, the despeckled products' $sigma_0$ values were not finally used in the correlation models and the unfiltered products were used instead.

Lee Sigma speckle filter

The Lee Sigma filter proposed by Lee et al. (1983), assumes Gaussian noise distribution and filters the center pixel in a sliding window with the average of pixels within the two-sigma range. One major drawback of the algorithm is that the mean of pixels within the two-sigma range is always underestimated due to the fact that the noise distributions are not symmetric and the symmetric thresholds are used in the pixel selection.

Refined Lee speckle filter

The refined Lee filter is a minimum mean square error (MMSE) filter and was developed based on the multiplicative noise model. One major deficiency with the MMSE filter is that speckle noise near strong edges is not adequately filtered. To compensate this problem, the refined Lee filter uses a nonsquare window to match the direction of edges. The filter operated in a 7x7 sliding window. One of eight edge-aligned windows is selected to filter the center pixel. Only the pixels in the non-edge area in the edge-aligned window are used in the filtering computation.

The filter follows three major processing steps as given below:

Edge-aligned window selection: For each pixel, span image is used in selecting the edge-aligned window.

Filtering weight computation: The local statistical filter is applied to the span image to compute the weight b.

Filter the covariance matrix: The same weight b (a scalar) and the same selected window are used to filter each element of matrix, Z, independently and equally. The filtered matrix is then given by

$$\hat{Z} = \overline{Z} + b\left(Z - \overline{Z}\right)$$

where,

$$\overline{Z}$$

is the local mean of matrices computed with pixels in the same edge-directed window.

4. Terrain correction

Due to topographical variations of a scene and the tilt of the satellite sensor, distances can be distorted in the SAR images. Image data not direct at the sensor's Nadir location usually have some distortion. Terrain corrections are intended to compensate for these distortions so that the geometric representation of the image will be as close as possible to the real world. Terrain Correction also allows geometric overlays of data from different sensors and/or geometries. For the geometric correction of the 2 GRD products, the Range Doppler Terrain Correction Operator was applied.

The geometry of topographical distortions in SAR imagery is shown below. Point B with elevation h above the ellipsoid is imaged at position B' in SAR image, though its real position is B". The offset Δr between B' and B" exhibits the effect of topographic distortions.

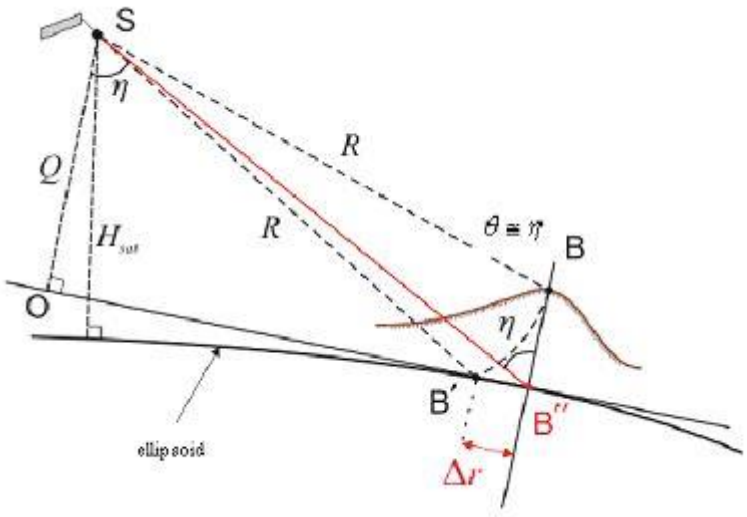

Εικόνα 3. Geometry of topographical distortions in SAR imagery. Source: SNAP Help.

Orthorectification Algorithm

The Range Doppler Terrain Correction Operator implements the Range Doppler orthorectification method [Small et al., 2008] for geocoding SAR images from single 2D raster radar geometry. It uses available orbit state vector information

in the metadata, the radar timing annotations, the slant to ground range conversion parameters together with the reference DEM data to derive the precise geolocation information. The DEMs used for the geometric correction of both the GRD products were 3 sec SRTMs which were auto downloaded.

5. Spatial subset

Spatial subsets of both the ascending and the descending passes were created, focused on the 4 study sites. The resulted products are shown in the maps below.

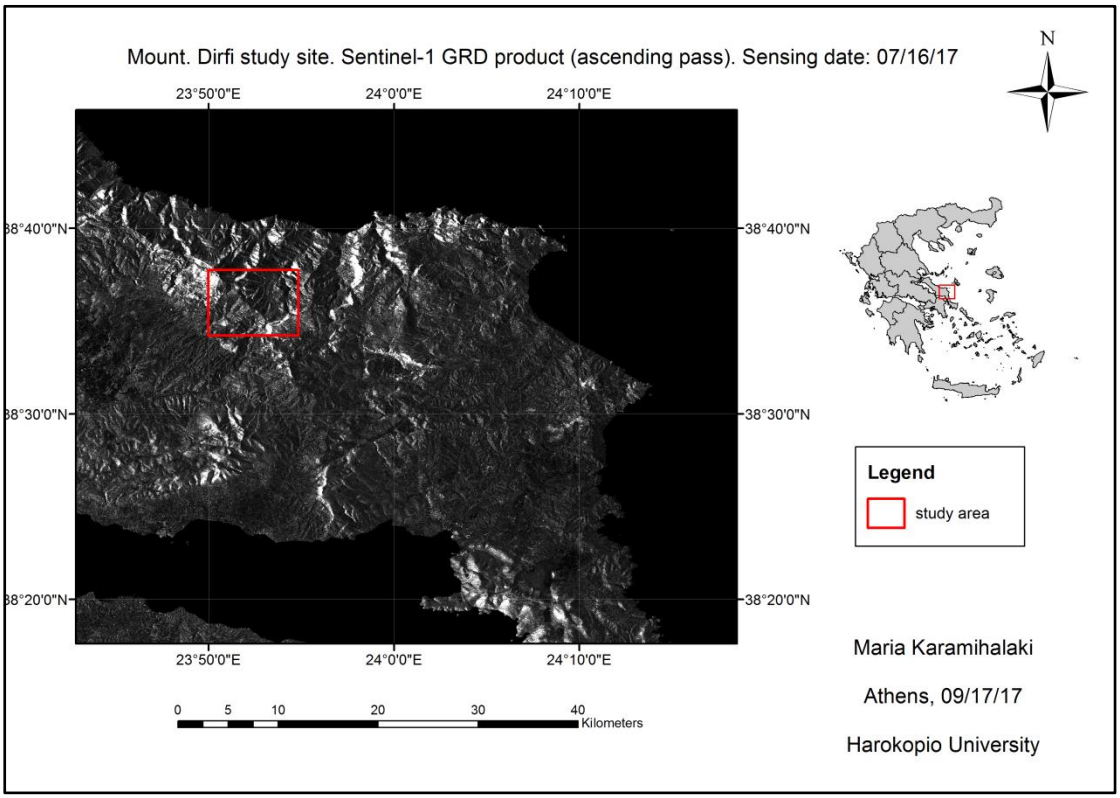

Map 1. Mount. Dirfi study site. Sentinel-1 GRD product (ascending pass). Sensing date: 07/16/17.

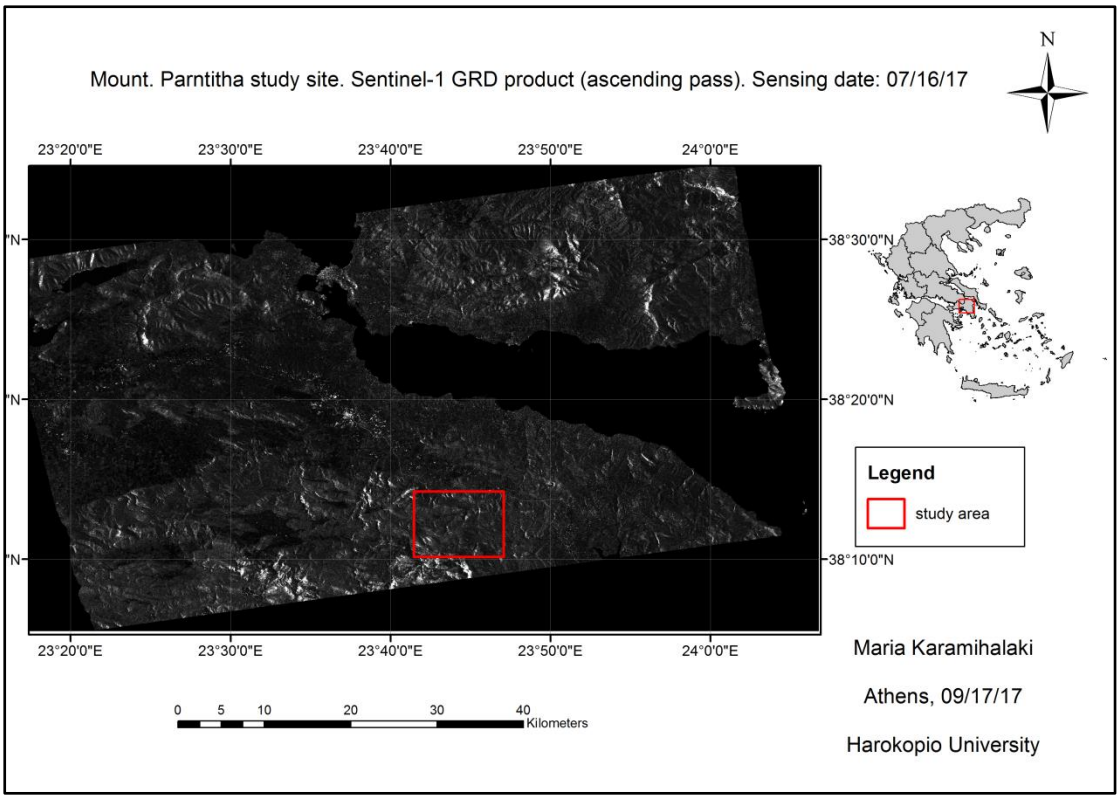

Map 2. Mount. Parntitha study site. Sentinel-1 GRD product (ascending pass). Sensing date: 07/16/17.

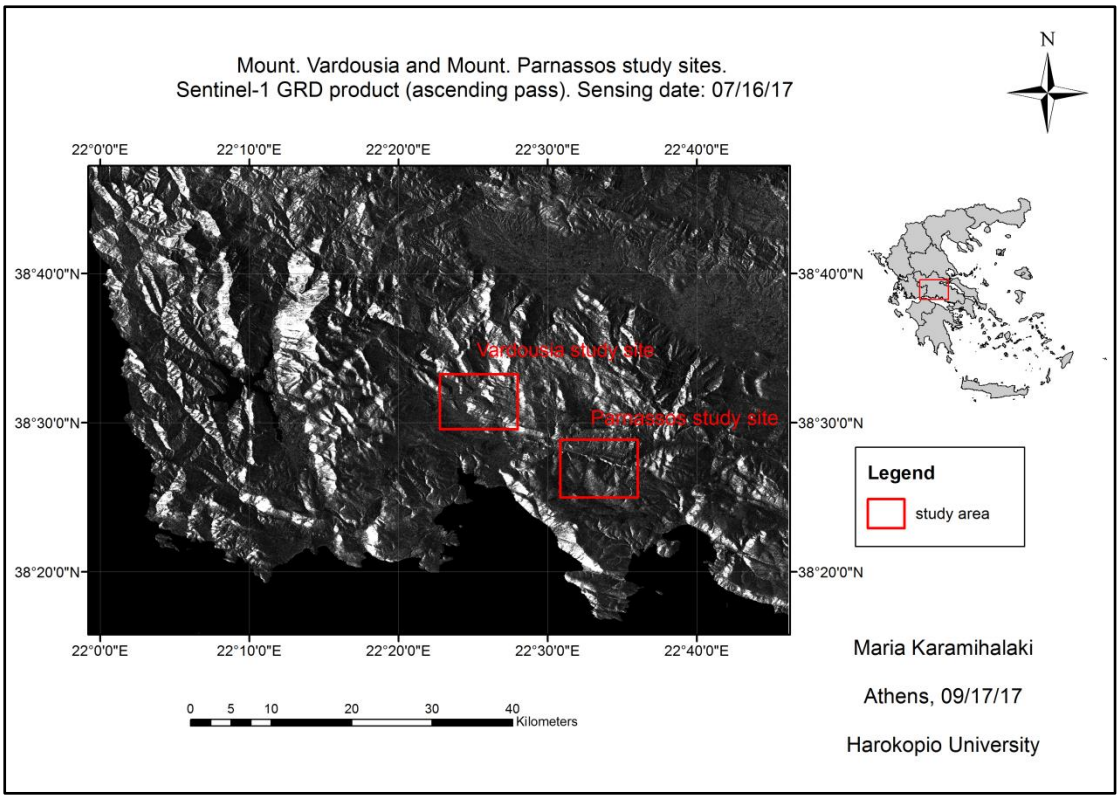

Map 3. Mount. Vardousia and Mount. Parnassos study sites. Sentinel-1 GRD product (ascending pass). Sensing date: 07/16/17.

6. Values extraction

Subsequently, the spatial subsets were exported in Geotiff format and the commercial remote sensing software ENVI was used for the extraction of the SAR backscatter coefficient values. In particular, pixel information was collected for 3x3 pixel windows that correspond to the study areas. The average value of each pixel window was then estimated; these values were finally taken into account for the correlation between SAR backscatter coefficient and AGB.

For the study site located in Parnitha, the coordinates of all four points that define each plot were taken, using a GPS device. That allowed the detection of the exact position of the sample plots, on the satellite images (with respect to the GPS error of about 3 meters). Thus, pixel information referring to the 3 sample plots in the study area of Parnitha corresponds to the exact positions where the field measurements were taken.

On the contrary, pixel windows corresponding to the sample plots of the study sites in Vardoysia, Parnassos and Dirfi, were chosen approximately, based on the point coordinates that were provided along with the biomass data from our colleagues for the FRI.

6.3.3. Empirical models

The establishment of a relationship between two variables requires an at least sufficient sample, in order for the resulted relationship to be considered reliable. As the sample data collected in the field could not be considered sufficient, two empirical models, found through the literature, were used in order to study the relationship between in-situ estimated AGB of mountainous Mediterranean conifer forests and C – band SAR backscatter coefficient. As these models have been developed for different types of vegetated ecosystems, they were calibrated with the *in situ* data that refer to the Mediterranean conifer forests of *A. cephalonica*.

In the first instance, the regression model developed by Suzuki et al. (2013) was used. For the purposes of their study, they examined the relationship between *in situ* forest AGB for 45 vegetated areas in Alaska (both forest and non-forest) and L – band σ^0. The resulted strong correlation between HV σ^0 and *in situ* forest AGB, allowed the robust estimation of forest AGB of the relatively sparse Alaskan boreal forest and the mapping of its geographic distribution. According to the proposed model, AGB can be estimated as shown below:

$$AGB = \exp[(\sigma^0+b)/ a] \quad (1)$$

This is the inverse of the regression function of σ^0 to the *in situ* forest AGB (equation 2). This regression function was used in order to examine the relationship between the *A. cephalonica* AGB and the SAR backscatter coefficient. The equation is provided below:

$$\sigma^0 = a \log x - b \quad (2)$$

where,

σ^0 is the SAR backscatter coefficient, *x* is the *in situ* biomass and *a* and *b* are the parameters estimated by the regression model.

In particular, the following relationships were examined, with the use of equation 4:

Linear relationship between: (a) ascending pass VH σ^0, (b) descending pass VH σ^0, (c) ascending pass VV σ^0, (d) descending pass VV σ^0 and the log transformed values of the (a) AGB(1), (b) AGB(2).

Subsequently, a second empirical model, developed by Chang and Shoshany (2016), was applied. In their study, they suggest a fusion model which combines optical and SAR data, for the development of a regression model for biomass estimation of Mediterranean shrublands. In particular, the proposed model combines two equations of the same form; in the first equation they use NDVI values (derived by Sentinel – 2 data) and in the second one, they use the SAR backscatter coefficient (derived by Sentinel – 1 data).

The model is of the same form with the model developed by Suzuki et al. (2013), except, they use the untransformed values of AGB.

For the purposes of the current study, the linear regression model proposed by Chang and Shoshany (2016), was applied, using the SAR backscatter coefficient values and the *in situ* biomass data.

The equation is provided below:

$$x = a + b\sigma^0 \quad (3)$$

where,

σ^0 is the SAR backscatter coefficient, x is the *in situ* biomass and a and b are the parameters estimated by the regression model.

In particular, the following relationships were examined, with the use of equation 3:

Linear relationship between: (a) ascending pass VH σ^0, (b) descending pass VH σ^0, (c) ascending pass VV σ^0, (d) descending pass VV σ^0 and the and (a) AGB(1), (b) AGB(2).

The data values used in the regression models are shown in the table below:

	Ascending VH	Ascending VV	Descending VH	Descending VV	AGB(1) (Mg/ha)	AGB(2) (Mg/ha)
Parnitha1	-16,65537278	-11,15753689	-15,0481338	-10,2949776	102,96	121,13
Parnitha2	-13,592081	-7,811281667	-13,1369115	-8,179623167	94,81	103,38
Parnitha3	-16,32693489	-5,979175556	-12,93704414	-6,219308857	107,58	127,11
Dirfi1	-12,00480578	-9,352699222	-13,42679789	-10,35435722	-	-
Dirfi2	-10,10904244	-4,703080333	-17,8015	-12,85661467	-	-
Parnassos1	-15,42265956	-10,55310333	-12,96832588	-7,41451075	-	-
Parnassos2	-10,21885	-7,223914778	-14,45900771	-9,253102429	-	-
Vardousia	-12,73585189	-7,629959333	-12,18725967	-6,803995444	-	-

Table 4. Values used in the regression models.

7. Results

This study discusses a first, preliminary approach on the relationship between C – band SAR backscatter coefficient ($sigma_0$) and AGB of mountainous Mediterranean conifer forests of *A. cephalonica*. Firsts results demonstrate the existence of a moderate relationship between the VH polarized SAR backscatter coefficient, of the ascending pass of the satellite, and the AGB, while no significant relationship is found between either the VV polarized SAR backscatter coefficient of both passes, or the VV polarized SAR backscatter of the descending pass and the AGB. More specifically, the stronger relationship indicated in this study is the logarithmic relationship that appears between the VH polarized SAR backscatter coefficient of the ascending pass and AGB(1) (R^2 = 0.2751). The simple linear relationship found between the VH polarized SAR backscatter coefficient of the ascending pass and the AGB(1), presents a correlation of moderate strength as well (R^2 = 0.204). Furthermore, another correlation of about the same magnitude is found between the VH polarized SAR backscatter coefficient of the ascending pass and the logarithm of the AGB(2) (R2 = 0.228), while a slightly weaker relationship results from the simple linear regression between the VH polarized SAR backscatter coefficient of the ascending pass and the AGB(2), using the abovementioned regression model (R^2 = 0.1756).

The results of all the weak correlations between SAR backscatter coefficient of different passes and polarizations and the AGB are provided in the appendix.

The scatterplots for the moderately strong relationships found in this study, are provided below.

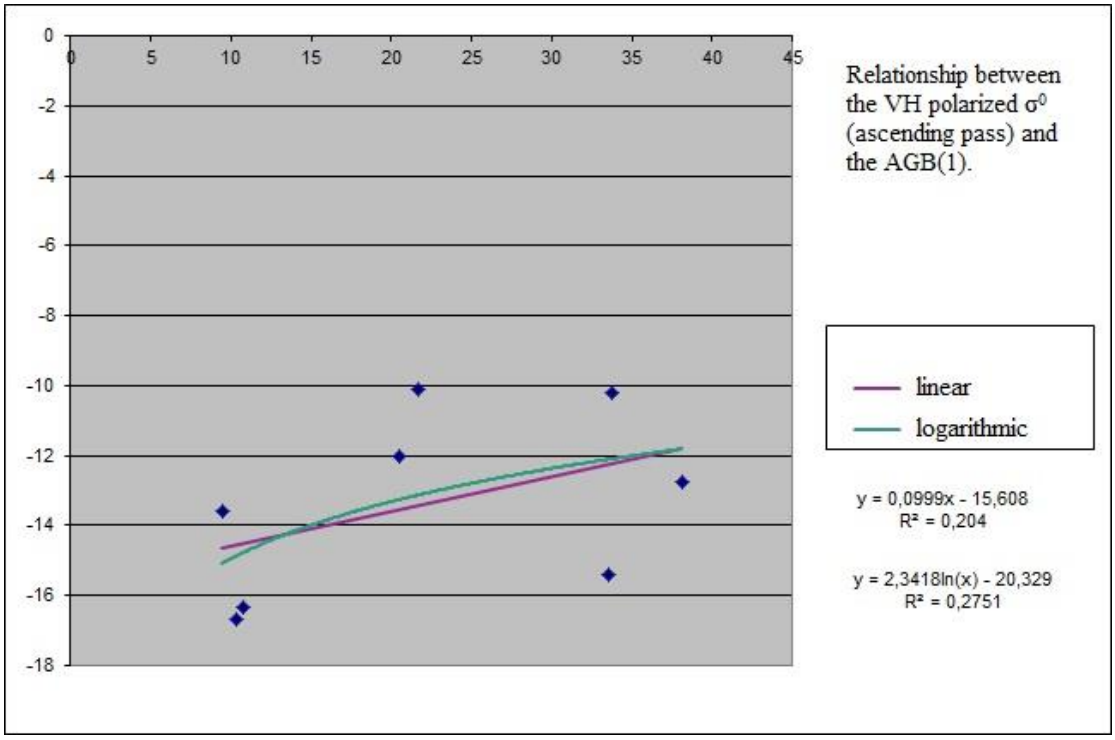

Figure 14. Relationship between the VH polarized σ^0 (ascending pass) and the AGB(1).

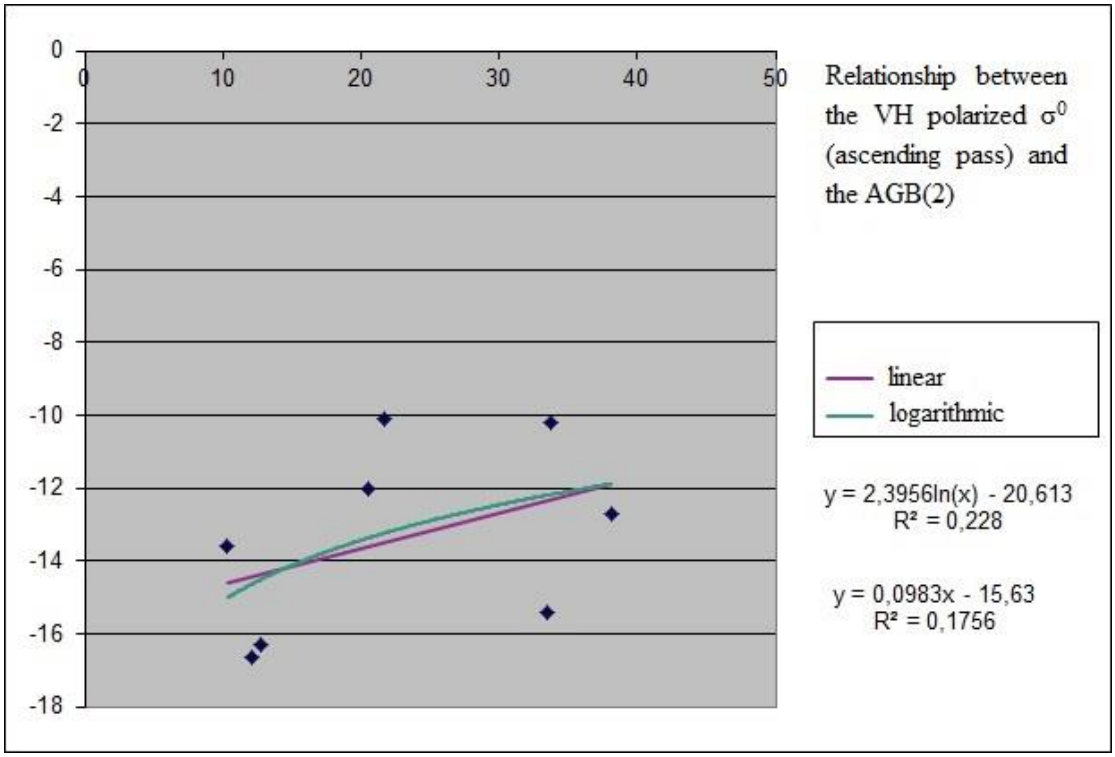

Figure 15. Relationship between the VH polarized σ^0 (ascending pass) and the AGB(2).

8. Discussion

Scientific methodology encompasses errors; recognizing the existence of those errors however and taking under consideration the limitations put by them is a key parameter in order to read between the lines, when interpreting the results of the adopted approach, in a study. In this direction, it is important to showcase the sources of error and the limitations that arise from the methods and the materials used in this study.

As mentioned before, this study constitutes a preliminary approach on the relationship between radar backscatter coefficient and AGB. As quoted by Rodríguez-Veiga et al. (2017), these approaches face several challenges, such as lack of sufficient ground data for calibration/validation purposes, signal saturation in high AGB, coverage of the sensor and complex signal retrieval due to topography. Challenges and limitations however, go beyond the satellite data. In this chapter, all sources of errors driven by the current study are being discussed.

In order to make an indirect estimation of an amount or the intensity of a phenomenon, a number of assumptions have to be made. To begin with, some first assumptions and limitations in this study, concern the field measurements. A first source of errors, regarding those measurements, is the GPS accuracy. The σ^0 values for the sample plots in the study area of Mount. Parnitha were extracted by pixels that were detected on the satellite images, according to the GPS positions. The position of the sample plot for the study sites in Vardousia, Parnassos and Dirfi was even vaguer. Another assumption made concern the biomass allometric equations used. Allometric equations allow an indirect estimation of the AGB. What is more, the allometric equations have been developed for the relative species *Abies alba.* Finally, the biggest source of uncertainty in this study is the limited sample of *in situ* measurements.

According to the results showcased in this study, it is concluded that both the polarization and the acquisition geometry affect the interaction of C – band SAR sensors with forest biomass (for the studied species). It has to be mentioned, that as the effect of the acquisition geometry, is related to the topography of the study site, sites with different topographical characteristics may present different behavior, regarding the acquisition geometry.

9. Conclusion

The initial question that triggered this study is whether it is possible to estimate and monitor the CO_2 that is accumulated in the biomass of mountainous Mediterranean conifer forests from space, by means of remote sensing. Monitoring carbon stocks of terrestrial ecosystems from space is already being practiced by the research community, over the last years, for a plethora of different vegetated ecosystems and species, mainly concerning boreal and tropical forests, as these two categories of forest ecosystems constitutes the main carbon stocks of terrestrial biomass. However, Mediterranean forests and other types of terrestrial vegetated ecosystems have less extensively been studied in terms of their carbon uptake capacity. There is of course a significant amount of studies regarding shrublands, agricultural ecosystems, Mediterranean conifers, etc. (e.g. Galidaki et al., 2016) found in the literature; it is important however, to start building knowledge on *species – specific* and *ecosystem – specific* methods and practices that can be used for the monitoring of terrestrial carbon stocks and the assessment of different types of vegetated ecosystems, regarding their carbon uptake capacity. *Species – specific* approaches on this subject are essential, as the carbon uptake differs between different species/ ecosystems. This differentiation has two aspects; firstly, there is a need for development of biomass allometric equations for every single species that has a relative importance in terms of its carbon uptake capacity. Hopefully, there is a great amount of biomass allometric equations, available to the scientific community; online databases, such as the *"GlobAllomeTree"*[24], consist an important contribution, along with the amount of published studies concerning this issue and the published reviews that provide a summary of the allometric equations available (e.g. Forrester et al., 2017). However, these collections are far from complete and further research is needed on this subject. Secondly, there is the aspect of the remote sensing approach, with regard to the different structural characteristics of different types of species and ecosystems, in terms of SAR data – based monitoring techniques. As SAR – based biomass monitoring techniques are highly dependent on the determination of the patterns of the interaction between the backscatter of the SAR signal and the structural characteristics of the canopy, the orientation and the surface of the leaves, the vegetation density, the characteristics of the background and the topographic characteristics of the study area, it becomes clear that *ecosystem/ species – specific* models have to be developed in order for the research community to obtain the capacity to monitor the CO_2 of the terrestrial vegetated ecosystems over the globe.

[24] http://www.globallometree.org/

As mentioned earlier, in order to procced to the modeling and mapping of the carbon uptake of a vegetated ecosystem, with the use of satellite derived parameters, the relationship between those parameters and the AGB needs to be established, for certain types of ecosystems. In this study, a preliminary approach was attempted on the relationship between C-band SAR backscatter coefficient and the AGB. The results suggest that the a moderately strong relationship is found between the VH polarized σ_0 of the ascending pass, an outcome that agrees with the general trends shown through the literature. However, our understanding of the relationship between the C-band SAR backscatter coefficient and the AGB of *A. alba ecosystems* is far from complete, due to the limitations that were previously described. Among all the limitations discussed here, the one with the greatest impact on the outcome, in terms of lack of reliability, is the sample size. Nevertheless, it is suggested that the methodology proposed in this study could provide a reliable outcome, that would set the foundation for carbon modeling of Mediterranean *A. alba* ecosystems, when a sufficient sample of *in situ* data would be available. The proposed methodology could be furtherly improved, by taking into account the limitations that were previously discussed, and by suggesting and applying improvements on them.

10. Future work

This is an ongoing study; further research on the subject and improvements regarding the limitations discussed above will be taken into consideration, in order to form more comprehensive conclusions on the relationship between SAR backscatter coefficient and ABG of mountainous Mediterranean forests. More importantly, a number of sample plots from different study sites are about to be added, which are expected to enhance the results of the current study. Furthermore, the study of the relationship between the AGB and parameters derived by different types of satellite data consists a promising approach on the subject and is about to be explored through future studies.

11. Bibliography

Amthor, J. S., & Baldocchi, D. D. (2001). Terrestrial higher plant respiration and net primary production. Terrestrial global productivity, 33-59.

Bombelli, A., Avitabile, V., Balzter, H., Belelli Marchesini, L., Bernoux, M., Brady, M., (…), Wulder, M. (2009) Biomass. In: di Caracalla VDT (ed) Assessment of the status of the development of the standards for the terrestrial essential climate variables (T12). Global Terrestrial Observing System, Rome.

Chave, J., Andalo, C., Brown, S., Cairns, M. A., Chambers, J. Q., Eamus, D., ... & Lescure, J. P. (2005). Tree allometry and improved estimation of carbon stocks and balance in tropical forests. Oecologia, 145(1), 87-99.

Cheng, Z., Gamarra, J. G. P., G. J., and Birigazzi, L. (2014). Inventory of allometric equations for estimating tree biomass – a database for China. UNREDD Programme, Rome, Italy.

Ciais, P., Dolman, A. J., Dargaville, R., Barrie, L., Bombelli, A., Butler, J., (...) & Moriyama, T. (2010). GEO carbon strategy. GEO Secretariat, Geneva/FAO, Rome.

Efthimiou, G., & Karageorgos, A. (2010). Biodiversity and Ecotouristic management study of the Steni Aesthetic Forest (GR24200002), Greece. In CD-ROM Proceedings of the International Conference Pre10: Protection and Restoration of the Environment X, University of Ioannina (UOI), Ioannina Greece and Stevens Institute of Technology (SIT) New Jersey USA (pp. 5-9).

Efthimiou, G., Detsis, V., & Theodoropoulou, O. (2014). Post fire forest restoration in a National Park: the Parnitha case, Greece. In Proceedings of the 12th International Conference on Protection and Restoration of the Environment, Skiathos Island, Grafima Publ., Thessaloniki, June (pp. 408-413).

Ferretti, A. (2014). Satellite InSAR data: reservoir monitoring from space. EAGE Publications.

Galidaki, G., Zianis, D., Gitas I., Radoglou K., Karathanassi V., Tsakiri-Strati, M., Woodhouse, I. & Mallinis, G. (2016). Vegetation biomass estimation with remote

sensing: focus on forest and other wooded land over the Mediterranean ecosystem. International Journal of Remote Sensing, 38(7) (pp. 1940-1966).

Ganas, A., Pavlides, S. B., Sboras, S., Valkaniotis, S., Papaioannou, S., Alexandris, G. A., ... & Papadopoulos, G. A. (2004). Active fault geometry and kinematics in Parnitha Mountain, Attica, Greece. Journal of Structural Geology, 26(11), 2103-2118.

Goetz, S. J., Baccini, A., Laporte, N. T., Johns, T., Walker, W., Kellndorfer, J., ... & Sun, M. (2009). Mapping and monitoring carbon stocks with satellite observations: a comparison of methods. Carbon balance and management, 4(1), 2.

Gould, S. J. (1966). Allometry and size in ontogeny and phylogeny. Biological Reviews, 41(4), 587-638.

Hedges, J. I. (1992). Global biogeochemical cycles: progress and problems. Marine chemistry, 39(1-3), 67-93.

Huang, W., Sun, G., Ni, W., Zhang, Z., & Dubayah, R. (2015). Sensitivity of multi-source SAR backscatter to changes in forest aboveground biomass. Remote Sensing, 7(8), 9587-9609.

Jagodzinski, A. M., Skorupski, M., Kasprowicz, M., Wojterska, M., Dobies, T., Kalucka, I., ... & Nowinski, M. (2011). Biodiversity of Greek fir (Abies cephalonica Loudon) experimental stands in Rogów Arboretum (Poland). Acta Scientiarum Polonorum. Silvarum Colendarum Ratio et Industria Lignaria, 4(10).

Jenkins, T. A., Mackie, E. D., Matthews, R. W., Miller, G., Randle, T. J., & White, M. E. W. (2011). FC Woodland Carbon Code: Carbon Assessment Protocol. Forestry Commission, Edinburgh.

Karamihalaki M., Sykioti O., Stagakis S. and Kyparissis A., (2015). Monitoring of vegetation ecosystems in Greece using vegetation indices time series. 10th International Congress of the Hellenic Geographical Society (Panhellenic and International Congresses Proceedings Collection, p. 881-892).

Kurz, W. A., & Apps, M. J. (2006). Developing Canada's national forest carbon monitoring, accounting and reporting system to meet the reporting requirements of the

Kyoto Protocol. Mitigation and Adaptation Strategies for Global Change, 11(1), 33-43.

Lei, D., Jingjuan, L., Guozhuang, S. (2008). Neural network-based analytical model for biomass estimation in Poyang lake wetland using ENVISAT ASAR data. The International Archives of the Photogrammetry, Remote Sensing and Spatial Information Sciences. Vol. XXXVII. Part B7.

Malhi, Y., Meir, P., & Brown, S. (2002). Forests, carbon and global climate. Philosophical Transactions of the Royal Society of London A: Mathematical, Physical and Engineering Sciences, 360(1797), 1567-1591.

Mermoz, S., Réjou-Méchain, M., Villard, L., Toan, T., Rossi, V. & Gourlet-Fleury, S. Decrease of L-band SAR backscatter with biomass of dense forests. Remote Sensing of Environment, Volume 159, 2015, p. 307-317.

Mitchard, E. T. A., Saatchi, S. S., Woodhouse, I. H., Nangendo, G., Ribeiro, N. S., Williams, M. Ryan, C. M., Lewis, S. L., Feldpausch, T. R. & Meir, P. (2009). Using satellite radar backscatter to predict above-ground woody biomass: A consistent relationship across four different African landscapes. Geophysical Research Letters, VOL. 36, L23401, doi:10.1029/2009GL040692, 2009.

Mitchell, A. L., Rosenqvist, A., & Mora, B. (2017). Current remote sensing approaches to monitoring forest degradation in support of countries measurement, reporting and verification (MRV) systems for REDD+. Carbon balance and management, 12(1), 9.

Patel, P., Srivastava, H. S., Panigrahy, S., & Parihar, J. S. (2006). Comparative evaluation of the sensitivity of multi-polarized multi-frequency SAR backscatter to plant density. International Journal of Remote Sensing, 27(2), 293-305.

Picard, N., Saint-André, L., & Henry, M. (2012). Manual for building tree volume and biomass allometric equations: from field measurement to prediction.

Politi, P. I., Georghiou, K., & Arianoutsou, M. (2011). Reproductive biology of Abies cephalonica Loudon in Mount Aenos National Park, Cephalonia, Greece. Trees, 25(4), 655-668.

Raftoyannis, Y., Spanos, I., & Radoglou, K. (2008). The decline of Greek fir (Abies cephalonica Loudon): relationships with root condition. Plant Biosystems, 142(2), 386-390.

Rodríguez-Veiga, P., Wheeler, J., Louis, V., Tansey, K., & Balzter, H. (2017). Quantifying Forest Biomass Carbon Stocks From Space. Current Forestry Reports, 3(1), 1-18.

Sandberg, G., Ulander, L. M., Fransson, J. E., & Soja, M. J. (2012, July). Measurements of forest change using P-band SAR backscatter. In *Geoscience and Remote Sensing Symposium (IGARSS), 2012 IEEE International* (pp. 1652-1655). IEEE.

Samaras, D. A. (2012). The vegetation of Greek fir (Abies cephalonica Loudon) forests on the Oxia-North Vardousia mountain system, central Greece, in relation to drought. Diss. Universität Freiburg.

Sinha, S., Jeganathan, C., Sharma, L. K., & Nathawat, M. S. (2015). A review of radar remote sensing for biomass estimation. International Journal of Environmental Science and Technology, 12(5), 1779-1792.

Small, D., & Schubert, A. (2008). Guide to ASAR geocoding. Issue, 1(19.03), 2008.

Suzuki, R., Kim, Y., & Ishii, R. (2013). Sensitivity of the backscatter intensity of ALOS/PALSAR to the above-ground biomass and other biophysical parameters of boreal forest in Alaska. Polar Science, 7(2), 100-112.

Svoray, T., Shoshanym M., Curran, P. J., Foody, G. M. & Perevolotsky, A. (2001) Relationship between green leaf biomass volumetric density and ERS-2 SAR backscatter of four vegetation formations in the semi-arid zone of Israel, International Journal of Remote Sensing, 22:8, 1601-1607.

Swingland, I. R. (Ed.). (2013). Capturing carbon and conserving biodiversity: The market approach. Routledge.

Appendix: additional charts

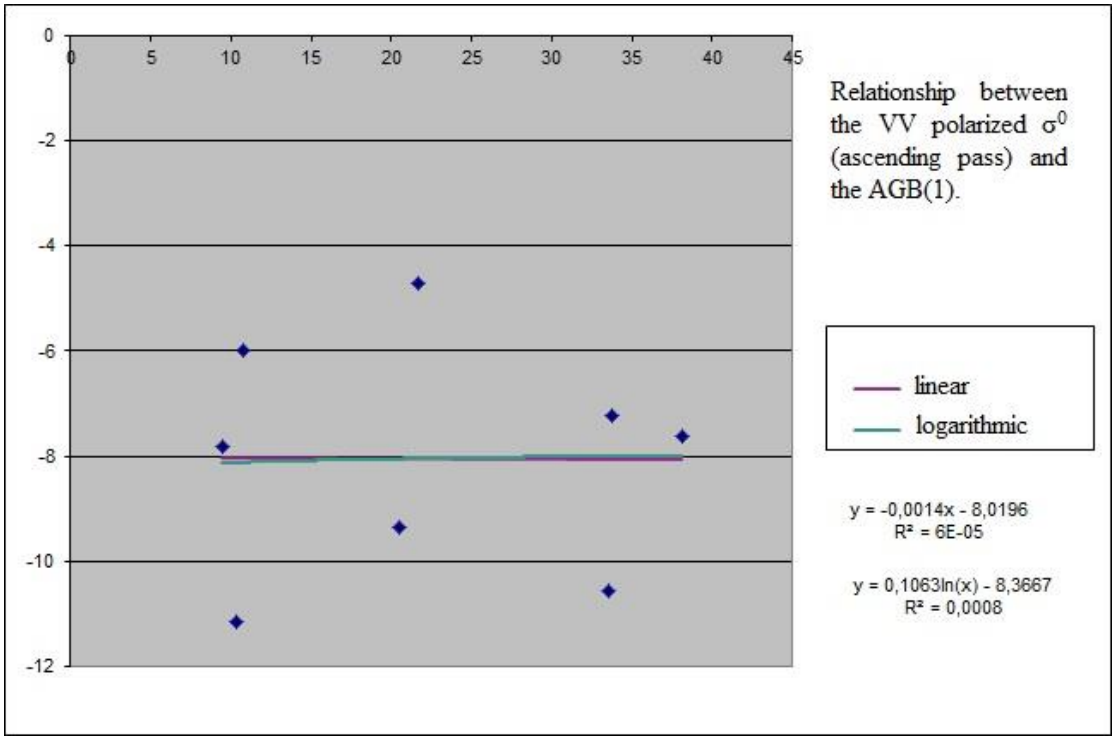

Relationship between the VV polarized σ^0 (ascending pass) and the AGB(1).

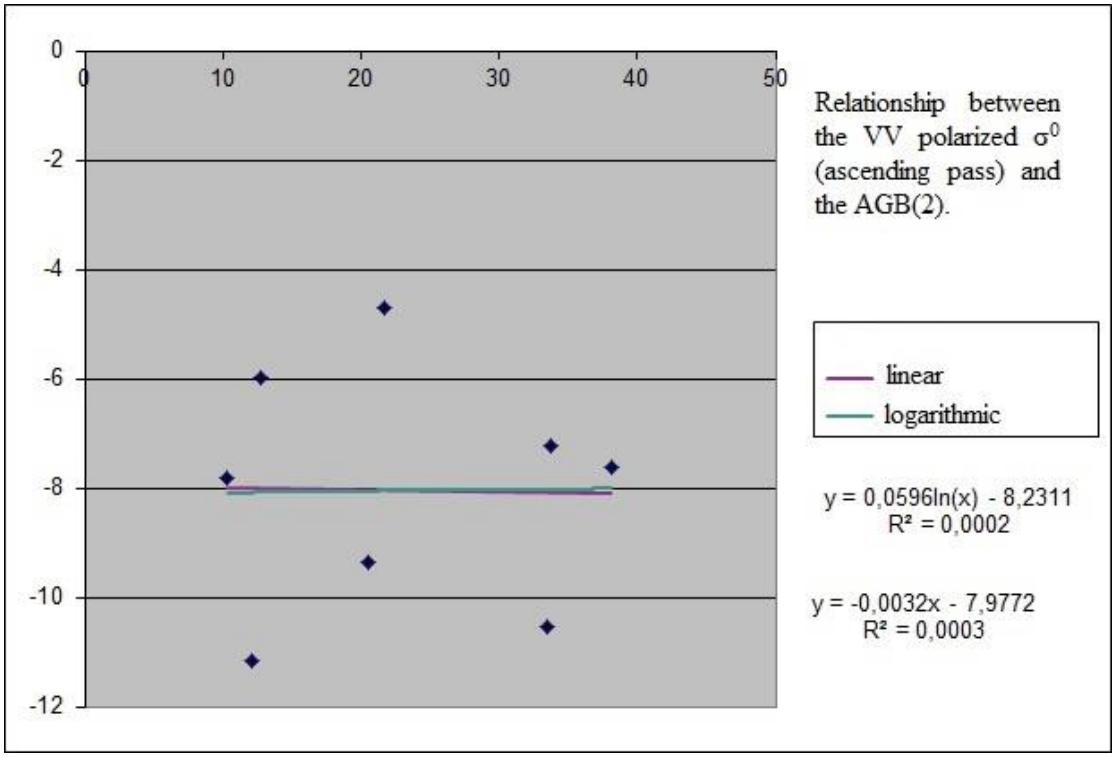

Relationship between the VV polarized σ^0 (ascending pass) and the AGB(2).

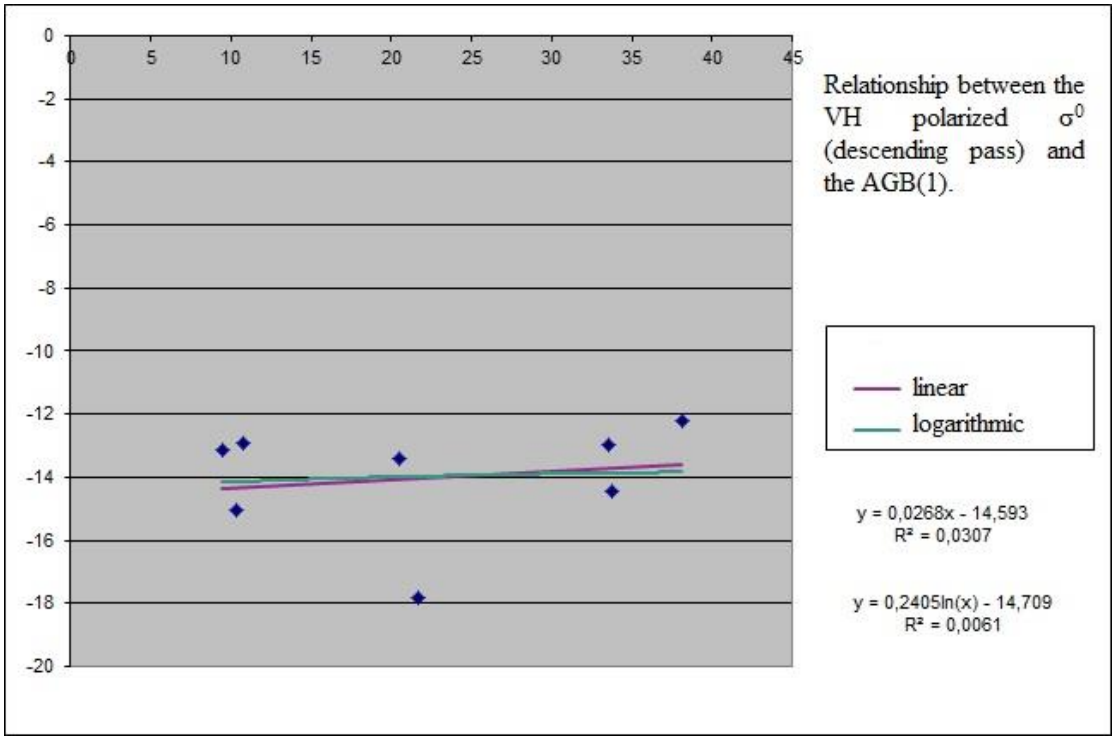

Relationship between the VH polarized σ^0 (descending pass) and the AGB(1).

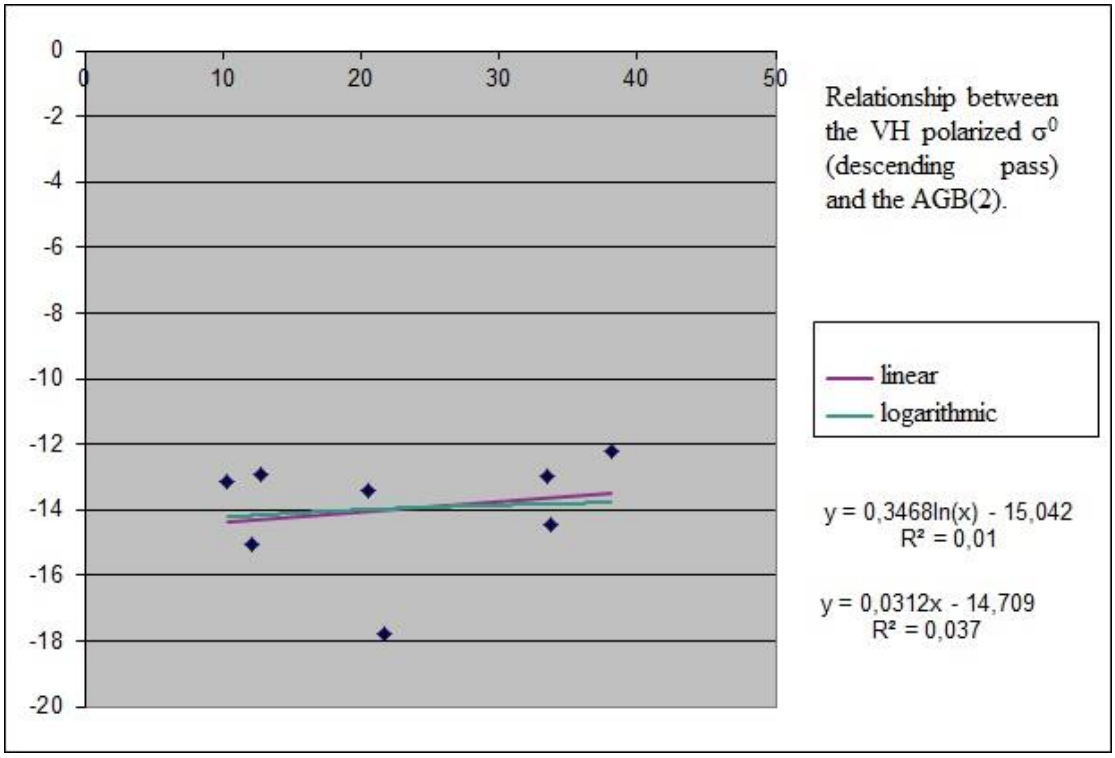

Relationship between the VH polarized σ^0 (descending pass) and the AGB(2).

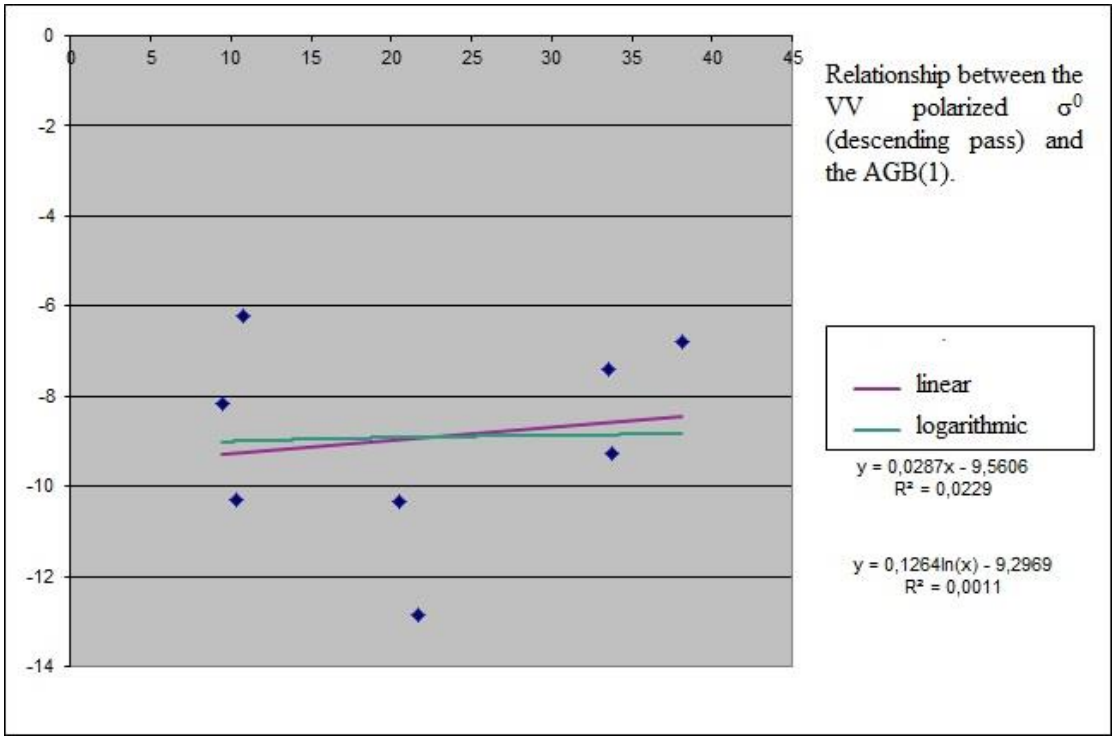

Relationship between the VV polarized σ^0 (descending pass) and the AGB(1).

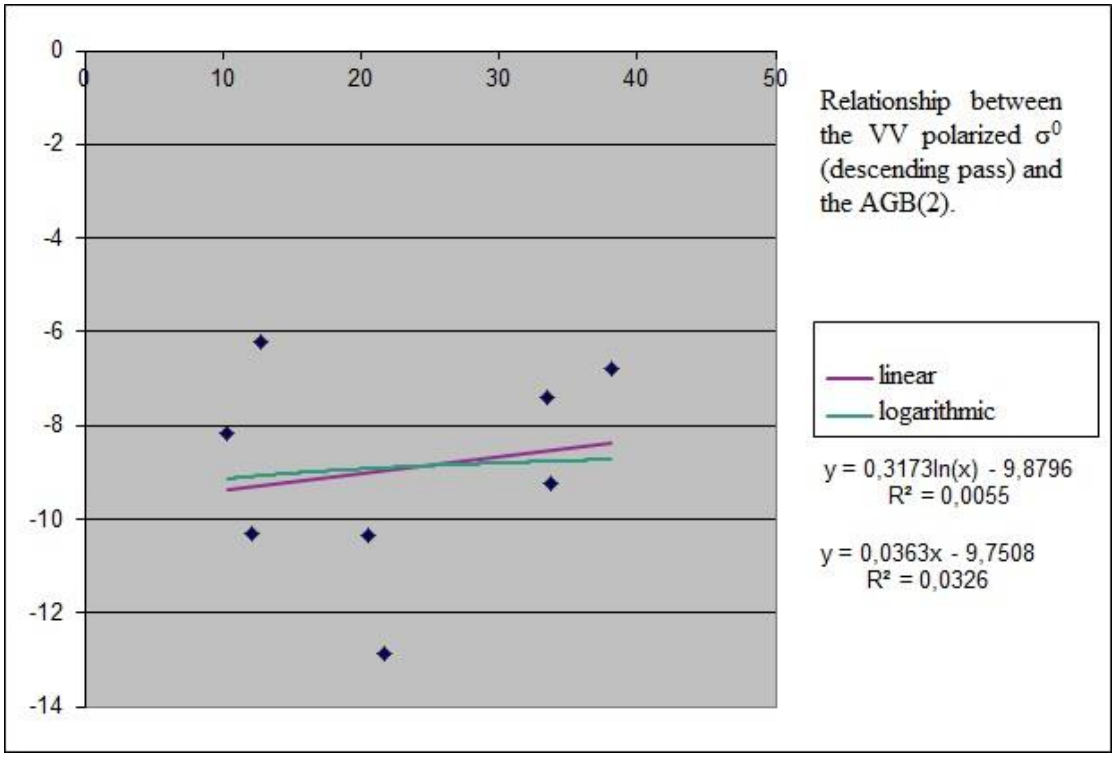

Relationship between the VV polarized σ^0 (descending pass) and the AGB(2).